Review in Advance first posted online on April 18, 2016. (Changes may still occur before final publication online and in print.)

Mechanics and Single-Molecule Interrogation of DNA Recombination

Jason C. Bell* and Stephen C. Kowalczykowski

Department of Microbiology and Molecular Genetics, and Department of Molecular and Cellular Biology, University of California, Davis, California 95616; email: sckowalczykowski@ucdavis.edu

Annu. Rev. Biochem. 2016. 85:27.1–27.34

The *Annual Review of Biochemistry* is online at biochem.annualreviews.org

This article's doi: 10.1146/annurev-biochem-060614-034352

*Present address: Department of Biochemistry, Stanford University, Stanford, California 94305

Keywords

helicase, DNA repair, RecA/RAD51, BRCA2, microscopy, visual biochemistry

Abstract

The repair of DNA by homologous recombination is an essential, efficient, and high-fidelity process that mends DNA lesions formed during cellular metabolism; these lesions include double-stranded DNA breaks, daughter-strand gaps, and DNA cross-links. Genetic defects in the homologous recombination pathway undermine genomic integrity and cause the accumulation of gross chromosomal abnormalities—including rearrangements, deletions, and aneuploidy—that contribute to cancer formation. Recombination proceeds through the formation of joint DNA molecules—homologously paired but metastable DNA intermediates that are processed by several alternative subpathways—making recombination a versatile and robust mechanism to repair damaged chromosomes. Modern biophysical methods make it possible to visualize, probe, and manipulate the individual molecules participating in the intermediate steps of recombination, revealing new details about the mechanics of genetic recombination. We review and discuss the individual stages of homologous recombination, focusing on common pathways in bacteria, yeast, and humans, and place particular emphasis on the molecular mechanisms illuminated by single-molecule methods.

Contents

INTRODUCTION

Homologous Recombination Is a Quiet Guardian of Genome Stability

During normal cell division, the genome must be accurately duplicated and segregated to each daughter cell. Abnormal cells that fail to faithfully complete this task exhibit a broad range of chromosomal aberrations, referred to as genomic instability, that include an accelerated frequency of mutations, DNA rearrangements, and aneuploidy. DNA is continuously exposed to metabolic

HOMOLOGOUS RECOMBINATION, CANCER, AND AGING

Inherited mutations in homologous recombination (HR) genes cause cancer predisposition and accelerated aging syndromes (3). Familial breast and/or ovarian cancer arise from mutations in *BRCA1* or *BRCA2*, which function independently to promote HR through DNA damage signaling and recombination initiation (BRCA1) or by chaperoning RAD51 to replication protein A (RPA)–coated single-stranded DNA (ssDNA) (BRCA2). Bloom's syndrome—caused by mutations in the *BLM* gene, one of the five human RecQ helicases—is exquisitely rare with only 265 cases recorded (4) and is a model for age-related cancers owing to a unique clinical pathology in which patients exhibit accelerated onset of nearly all cancer types (6). $BLM^{-/-}$ cells exhibit a 10-fold increased rate of sister chromatid exchanges (SCEs) due to a deficiency in dissolution of double Holliday junctions (dHJs) (6, 14). Fanconi's anemia (FA) is a rare genetic disorder associated with developmental abnormalities, bone marrow failure, and cancer predisposition (5). FA patients are predisposed to childhood or adolescent leukemias and have a median lifespan of 33 years. The disease arises from a hypersensitivity to DNA cross-linking agents, of which rapidly dividing hematopoietic cells are particularly susceptible. Approximately 15 genes have been identified in the FA pathway, and the tumor suppressor genes *BRCA1* and *BRCA2* have been linked to chromosomal instability suppression through promotion of HR-dependent cross-link repair (5).

and environmental factors that chemically damage the coding and continuity of chromosomes in the form of a range of lesions, including double-stranded DNA (dsDNA) and single-stranded DNA (ssDNA) breaks, inter- and intra-strand DNA cross-links, oxidative damage, and alkylation (1). The efficient detection and repair of these lesions requires a network of modular, flexible, and overlapping repair pathways to function throughout the cell cycle. Amazingly, most cells achieve this feat with incredible precision, accumulating only a single mutation after hundreds of cell divisions in the face of incredibly high levels of spontaneous DNA damage, on the order of 10,000 to 100,000 lesions per cell per day (1, 2). Persistent and chronic DNA lesions that remain unrepaired during DNA replication threaten both viability and fecundity by reducing genomic stability and causing mutations to accumulate. Genomic stress may be caused by chronic environmental exposure to clastogens; however, cells that are defective in their ability to repair DNA lesions disproportionately suffer genomic stress from normal metabolism. This is most clearly evident in the clinical and molecular pathology of developmental disorders, accelerated aging, and cancer-predisposition syndromes associated with impaired DNA repair and recombination (see **Table 1** and the sidebar, Homologous Recombination, Cancer, and Aging).

Homologous recombination (HR) maintains genomic integrity by pairing a damaged chromosome with an undamaged sister or homolog and using it as a template for DNA repair. HR has four core steps: (*a*) initiation, which is the resection of a damaged chromosome from a dsDNA break or an ssDNA gap; (*b*) presynapsis, which is the formation of the RecA or RAD51 filament on ssDNA; (*c*) synapsis, which is the pairing of sister chromatids or parental homologs catalyzed by either RecA or RAD51 filaments; and (*d*) postsynapsis, which can proceed through several alternative subpathways to uncouple joint molecules (**Figure 1**).[1] These postsynaptic pathways are of particular genetic importance because they determine whether paired chromosomes produce crossovers or noncrossovers (6).

Initiation: the process by which a damaged chromosome is resected through either the sole or coordinated action of nucleases and helicases to produce single-stranded DNA for the formation of a RecA or RAD51 filament

Presynapsis: the process by which RecA or RAD51 filaments form, respectively, on either SSB (ssDNA-binding protein)- or RPA (replication protein A)-coated single-stranded DNA

[1]Throughout this article, we have used the following convention for eukaryotic protein names: Names from *Saccharomyces cerevisiae* have only the first letter capitalized, whereas those from human have all letters capitalized. For cases in which the distinction is not important, only the human convention is used so as not to be overly tedious.

Table 1 Homologous recombination and human disease

Syndrome (references)	Primary genes and interaction partners	Pathway(s)	Clinical pathology	Molecular pathology	Prevalence
Fanconi's anemia (5, 159, 160)	*FANCA*, *FANCB*, *FANCC*, *FANCD1 (BRCA2)*, *FANCD2*, *FANCE*, *FANCF*, *FANCG (XRCC9)*, *FANCI*, *FANCJ (BRIP)*, *FANCL (PHF9)*, *FANCM*, *FANCN (PALB2)*, *FANCO (RAD51C)*, *FANCP (SLX2)*, *FANCR (RAD51)* (*FANCM* interacts with *FAAP24*; *FANCB* and *FANCL* with *FAAP100*)	Fanconi's anemia pathway, DNA cross-link repair, homologous recombination	Congenital abnormalities, bone marrow failure, sensitivity to DNA cross-linking agents, cancer predisposition (especially acute myeloid leukemia and solid tumors)	Increased frequency of binucleated cells and ultrafine chromatin bridges, increased cytokinesis failure, and increased chromosome instability, especially in the presence of DNA cross-linking agents	1 in 360,000 births; 1 in 200 carriers
Bloom's syndrome (150, 161)	*BLM* (interacts with *TOPOIIIα*, *RMI1/2*, *RPA*, *DNA2*, *RAD51*)	Homologous recombination	Short stature and congenital abnormalities, hypogonadism, hypersensitivity to sunlight, immunodeficiency, greatly elevated risk of all cancer types, especially carcinomas, leukemias, and lymphomas	10-fold increase in sister chromatin exchanges, quadriradial chromatids, defective Holliday junction dissolution or resolution pathways, ultrafine chromatin bridges	<300 cases reported; 1 in 40,000 among Ashkenazi Jews
Nijmegen breakage syndrome (162)	*NBS1* (interacts with *MRE11-RAD50*, *ATM*)	DNA damage response	Microcephaly, congenital abnormalities, immunodeficiency, radiation sensitivity, and cancer predisposition (especially lymphoid malignancies)	Low mitotic index in lymphocytes, radiation sensitivity, chromosome rearrangements	1 in 100,000 births

(*Continued*)

Table 1 (*Continued*)

Syndrome (references)	Primary genes and interaction partners	Pathway(s)	Clinical pathology	Molecular pathology	Prevalence
Familial breast and ovarian cancer (163–165)	*BRCA1*, *BRCA2*, *RECQ1* (*BRCA2* interacts with *RAD51*, *PALB2*, *EMSY*)	DNA damage response, homologous recombination	4- to 5-fold increase in lifetime risk of breast and ovarian cancer	Chromosomal instability, hypersensitivity to DNA damaging agents, defective RAD51 recruitment, DNA damage	1 in 400 births
Werner's syndrome (150, 166, 167)	*WRN* (interacts with *NBS1*, *MRN*, *Ku70/80*, *PARP1* *POT1–TRF1/2*, *FEN1*)	DNA replication, homologous recombination, base excision repair, telomere maintenance	Accelerated aging, including atherosclerosis, cataracts, gray hair, osteoporosis, type 2 diabetes; elevated risk of sarcomas	Delayed S-phase progression, sensitivity to DNA damage, accelerated telomere degradation, reciprocal translocations and extensive deletions; increased senescence can be overcome by telomerase overexpression	1 in 20,000 to 1 in 40,000 births
Ataxia–telangiectasia (168)	*ATM* (targets >700 proteins, including *BRCA1*, *MRE11*, *NBS1*, *FANCD2*, *SMC1*, *CHK2*, *p53*, *H2AX*, *53BP1*)	DNA damage response, double-strand break repair	Progressive neurodegenerative disease with telangiectasia, immunodeficiency, increased cancer risk, and radiation sensitivity	Chromosome instability, spontaneous DNA breaks, stable rearrangements	1 in 40,000 to 1 in 100,000 births
Rothmund–Thomson syndrome (150, 167, 169)	*RECQ4*, (interacts with *RPA*, *FEN1*, *PARP1*, *POLβ*)	Base excision repair, homologous recombination, DNA replication	Photosensitivity, poikiloderma (chronic rash), cataracts, gray hair, alopecia, short stature, skeletal abnormalities; elevated risks of osteosarcoma, basal cell carcinoma, and squamous cell carcinoma	Hematopoietic failure in mice, radiation sensitivity, defects in sister chromatid cohesion	<400 cases reported

Information compiled from Reference 158, except as noted.

In most genetic texts, recombination is synonymous with the allelic exchange occurring between parental chromosomes during meiosis (i.e., the shuffling of the genetic deck); however, it has long been appreciated that HR has a major role during replication (7, 8). In normally dividing *Escherichia coli*, stalled or broken replication forks must be reinitiated by recombination in 15–50% of cells, even under unstressed growth conditions (9, 10). Similarly in human cells, approximately 50 stalled or broken forks must be restarted—on average one per chromosome—during each

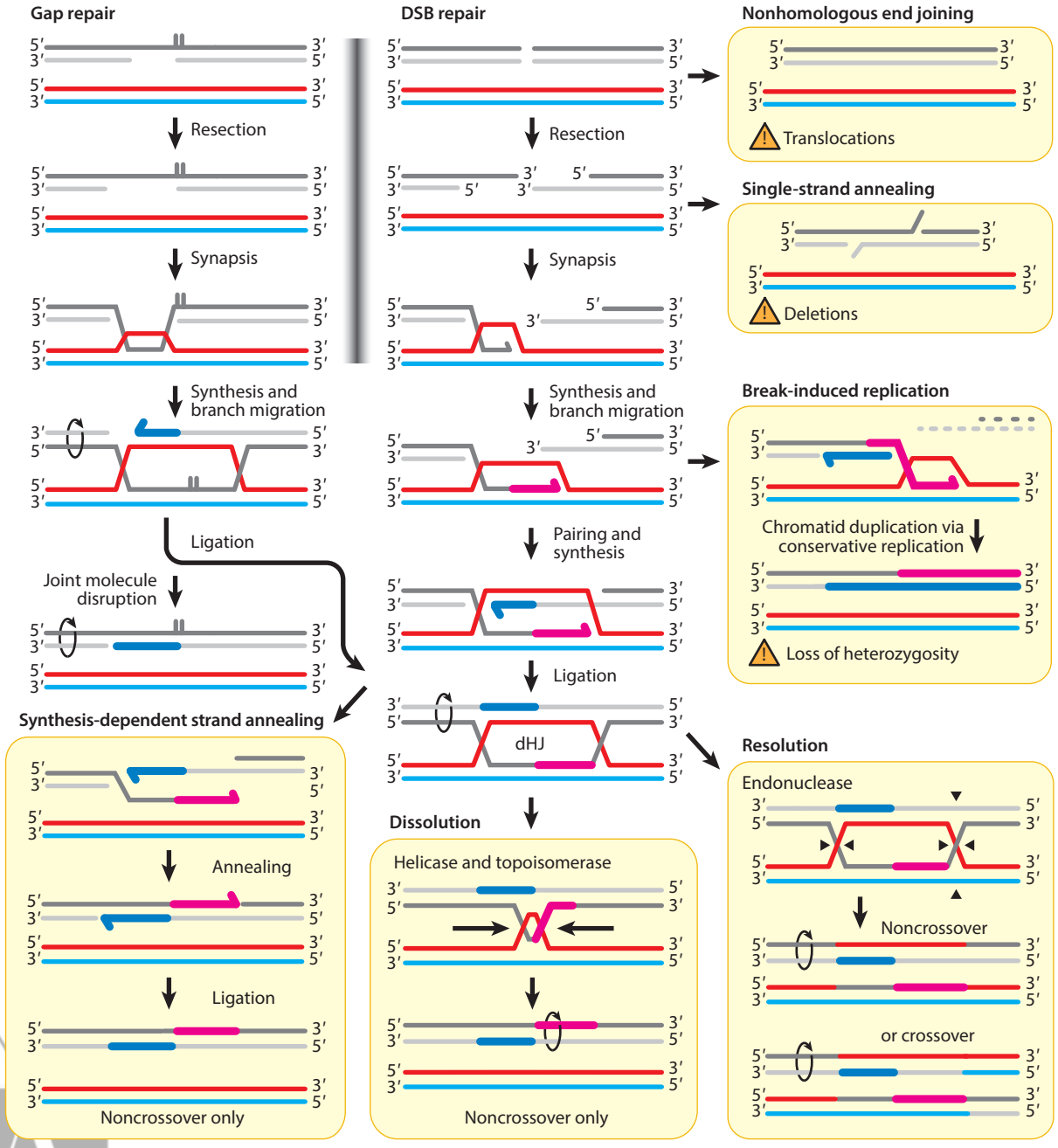

round of division (11). In this context, recombination is charged with the task of aligning and repairing a chromosome rather than promoting genetic diversity. Recombination proceeds through many stages of molecular gymnastics—including DNA unwinding, pairing, synthesis, annealing, and branch migration—to achieve chain continuity (**Figure 1**), and it may use a daughter chromosome, sister chromatid, or parental homolog. When recombination proceeds using a homolog, the consequence risked is allelic exchange and loss of heterozygosity. Alternatively, when recombination proceeds using either a daughter chromosome or sister chromatid, which are identical to the damaged chromosome, the repair can be both perfect and scarless, resulting in silent recombination. The sister chromatid is placed in space (either through sister chromatid cohesion or catenation, or both) and time to make it the most likely target of DNA pairing. Indeed, mitotically growing, budding yeast cells favor sister chromatid recombination with a 4:1 bias, in stark contrast to a 1:5 bias during meiosis (12). Silent recombination events are detectable cytogenetically by staining sister chromatids after bromodeoxyuridine (BrdU) incorporation, enabling the visualization and quantification of sister chromatid exchange (SCE) (13). In normal cells, the frequency of SCE is low, with approximately 2–10 exchanges per cell per division (14); however, this low frequency of SCEs is not due to the suppression of recombination initiation or pairing, but rather due to a unique molecular mechanism by which mitotic recombination intermediates are separated (6). The uncoupling of single and double Holliday junctions (HJs) proceeds through one of two mechanisms: dissolution, in which a double HJ (dHJ) is dissolved through concerted branch migration by either a DNA helicase or motor protein and unlinking by a type IA topoisomerase [e.g., BLM–TOPIIIα–RMI1–RMI2 (BTRR), *humans*], or resolution, in which an HJ or precursor is cut by one or several endonucleases (e.g., MUS81–EME1, SLX1–SLX4, or GEN1, *humans*) (**Table 2**). The dissolution pathway exclusively produces noncrossover products, but the resolution pathway may produce either crossover or noncrossover products (**Figure 1**) (6, 15).

Nearly 50 years ago, Clark & Margulies (16) identified the first recombination mutant (*recA*) in *E. coli*, initiating decades of elegant genetic dissection and biochemical characterization. It has only been during the past two decades that the clinical significance of homologous recombination in human cancers has become fully appreciated, but the rapid dissection of the molecular genetics of recombination in human cancers owes much to the significant body of work built around this small organism. Because of this connection, we have organized the functional homologs from *E. coli*, yeast, and humans according to their biochemical and genetic functions (**Table 2**) and

Synapsis: the process by which RecA or RAD51 filament searches for double-stranded DNA that is homologous to the sequence within the single-stranded DNA upon which the filament is formed, followed by pairing of the homologous sequence and displacement of the identical strand in the duplex

Postsynapsis: the process by which paired chromosomes are replicated and uncoupled

Silent recombination: recombination events occurring between sister chromosomes that result in repair using DNA that is identical in sequence and, hence, genetically silent

Figure 1

Recombination-mediated repair proceeds through many reversible and metastable intermediates. Daughter-strand gaps (*left*) formed by stalled replication forks are repaired by recombination. The single-stranded DNA (ssDNA) in the gap serves as the template for assembly of RecA or RAD51 and invades the intact chromosome (i.e., homologous pairing). After synapsis, the broken chromosome serves as the primer for DNA synthesis. Double-strand break (DSB) repair (*center*) proceeds by first resecting the break to produce an ssDNA overhang, typically with a 3′-terminated end on which RecA or RAD51 filaments assemble and then catalyze synapsis to form joint molecules. The 3′-end of the joint molecule serves as the primer for DNA synthesis. The other resected end of the DSB can either invade independently or can anneal to the displaced strand formed by the first extended joint molecules in a process termed second-end capture. The other 3′-end is extended by DNA polymerase. The joint molecules can be ligated, but do not need to be. This intermediate has two alternative fates: The joint molecule can be disrupted and the newly synthesized strands of the broken chromosome reanneal through a process termed synthesis-dependent strand annealing; alternatively, the two Holliday junctions (HJs) can persist and are uncoupled through either the dissolution or resolution pathway. The dissolution of a double HJ (dHJ) intermediate proceeds through the coordinated action of a RecQ-like helicase and a type IA topoisomerase and strictly results in noncrossovers. Resolution proceeds through endonucleolytic cleavage of the HJs, and produces both crossovers and noncrossovers; for clarity, only one of the two possible cuts is depicted in the left HJ. Alternative repair pathways (*right*) that also repair DNA breaks are nonhomologous end joining, microhomology-mediated end joining (not shown), single-strand annealing, and break-induced replication that proceeds by conservative DNA synthesis. These alternative pathways are intrinsically mutagenic.

Table 2 Functional groupings of recombination proteins for *Escherichia coli*, *Saccharomyces cerevisiae*, and humans

Organism	Resection	Single-stranded DNA binding	Mediators	Single-stranded DNA Annealing	DNA strand exchange	Branch migration	Dissolution or resolution
Escherichia coli	RecBCD RecQ RecJ	SSB	RecFOR RecOR	RecO	RecA	RuvA–RuvB RecQ UvrD	RecQ TopoIII RuvA–RuvB RuvC
Saccharomyces cerevisiae	Mre11–Rad50–Xrs2 Sae2 Sgs1–Dna2 Exo1	RPA	Rad52 Rad55–Rad57 Shu1–Shu2–Psy3–Csm2	Rad52	Rad51	Sgs1–Top3–Rmi1 Rad54 Rdh54 Mph1 Srs2	Sgs1–Top3–Rmi1 Mus81–Mms1 Slx1–Slx4 Yen1
Human	MRE11–RAD50–NBS1 CtIP WRN–DNA2 BLM–DNA2 EXO1	RPA	BRCA2 PALB2 SWS1–SWSAP1 SW5–SFR1 RAD51B–RAD51–RAD51D–XRCC2–XRCC3	RAD52	RAD51	BLM-TOPOIIIα–RMI1/2 RAD54 RAD54B FANCM RECQ1 WRN	BLM–TOPOIIIα–RMI1–RMI2 MUS81–EME1/EME2 SLX1–SLX4 GEN1

have presented a comparative review for each step in homologous recombination, with special emphasis on mechanisms illuminated by single-molecule experiments. For a more comprehensive and inclusive review of the biochemistry of recombination, we refer the interested reader to Reference 17.

Dissolution: the uncoupling of topologically linked double Holliday junctions through the combined action of either a DNA helicase or motor protein and a type IA topoisomerase

Resolution: the nucleolytic cleavage of a Holliday junction or Holliday junction precursor

Visual Biochemistry and Single-Molecule Spectroscopy: The Science of Watching Molecules Work

Recombination-based DNA repair has evolved as a mechanism to circumvent genomic catastrophe during cell division and proceeds through a kinetically regulated pathway of many reversible, metastable intermediates (18). The transient and stochastic nature of how these intermediates are formed and processed masks the dynamic behavior of each molecule that is critical to understanding the mechanics of homologous recombination. During the past two decades, the tools required to observe and manipulate single molecules have become increasingly available to molecular biologists (19–25). Broadly speaking, single-molecule methods aim to measure the dynamics of a protein, nucleic acid (DNA or RNA), or macromolecular assembly (i.e., protein complexes or nucleoprotein filaments). Single-molecule techniques typically use some combination of microscopy, micromanipulation or force measurement (e.g., using magnetic tweezers or optical traps), a microfluidic device to control or perturb the solution conditions, and some form of sensitive optical detection (usually fluorescence). The observation of single molecules moving

and working makes data interpretation remarkably direct; quite simply, often, "seeing is believing," making single-molecule methods powerful tools for reconciling seemingly contradictory functions and revealing complex biochemical behaviors that arise from the kinetic shuttling of intermediates.

With respect to single-molecule methods used to study homologous recombination, a handful of approaches are exceptionally useful (**Figure 2**). These methods fall broadly into three classes that we group as (*a*) direct spatial imaging of molecules—visual biochemistry—typically using epifluorescent or total internal reflection fluorescence (TIRF) microscopy; (*b*) temporal optical detection of molecules, typically using fluorescence methods such as single-molecule Förster resonance energy transfer (smFRET) or fluorescence correlation spectroscopy (FCS); and (*c*) mechanical detection of molecules by methods that comprise force spectroscopy. Visual biochemistry is a collection of single-molecule methods that use either epifluorescence or TIRF microscopy to directly image individual proteins usually bound to, and working on, much larger molecules, either alone or with partners. In visual biochemistry experiments, molecules are manipulated by rapidly changing the solution within a flow chamber—which can be a simple single-channel flow cell or a more complex microfluidic device—while immobilizing the molecule under observation (**Figure 2*a***). With a single optical trap, flow is typically used to extend the DNA molecule (26). To introduce the captured molecule to different solutions, a multichannel flow cell can be used to generate parallel laminar flows without physical boundaries between different solutions (27). By moving the flow cell (mounted to the stage) relative to the stationary optical trap, the molecule can be dipped into different solutions containing a protein of interest to, first, observe binding and, then, it can be transferred to another channel to initiate its activity (e.g., translocation) (19, 28, 29). Because a single molecule can be manipulated and observed for many minutes, several recursive measurements can be made of the same molecule under different conditions (30). When two or more optical traps are used, either both ends of the DNA molecule or multiple DNA molecules can be micromanipulated within the imaging plane in order to add a mechanical dimension to the experiment (**Figure 2*b***) (20).

An alternative imaging method uses TIRF microscopy to illuminate a thin optical plane above the glass surface of a flow cell (23, 25). In this way, a molecule of DNA can be tethered to the surface, and fluorescent proteins can be imaged as they bind to, move on, and dissociate from the DNA at concentrations normally too high for epifluorescence microscopy (**Figure 2*c***). To increase specificity and reduce background, surface attachment requires both functionalization and passivation using a polymer brush (e.g., polyethylene glycol), lipid bilayers, or protein adsorption (**Figure 2*d***) (31). By tethering the DNA to lipids within a surface-immobilized bilayer, flow can be used to push DNA molecules along the surface until they hit a fabricated nanobarrier, where they will accumulate into an ordered array called a DNA curtain, which allows for many more molecules to be simultaneously imaged (25).

TIRF microscopy can also be used to measure the Förster resonance energy transfer (FRET) between two fluorescence molecules in close proximity (i.e., <10 nm) (**Figure 2*e***) (32). Single-molecule FRET is used to monitor dynamic fluctuations of molecules immobilized on a surface (**Figure 2*f***), although they can also be confined in small volumes (e.g., lipid vesicles, droplets, or containment wells) (33). Single-molecule FRET has unparalleled precision and resolution, capable of monitoring nanometer-scale changes, and fluctuations on the millisecond timescale, directly reducing protein–DNA interactions into their most fundamental, digitized on-states and off-states, during binding, movement, and dissociation.

One of the earliest forms of single-molecule experiments with DNA used force spectroscopy, in which a molecule of DNA is tethered between either an immobile surface and an optical trap or a glass micropipette, or between two optical traps (21, 34). In the optical trap configuration,

Visual biochemistry: a class of single-molecule methods that directly images molecules using either epifluorescence or total internal reflection fluorescence (TIRF) microscopy

Single-molecule Förster resonance energy transfer (smFRET): an optical method that measures energy transfer from one fluorophore to another, used at the single molecule level to monitor and reduce single-molecular interactions into their most fundamental, digitized on-states and off-states, during binding, movement, and dissociation

Fluorescence correlation spectroscopy (FCS): an optical method that measures the Brownian diffusion of individual molecules by virtue of the correlated fluctuations in fluorescence intensity resulting from diffusion in and out of a small limited volume (e.g., ~1 fL)

Force spectroscopy: a class of single-molecule methods that typically uses sensitive physical, optical, or magnetic manipulation of a molecule, here DNA usually tethered to a bead, to measure either displacement under constant force or force exerted during displacement

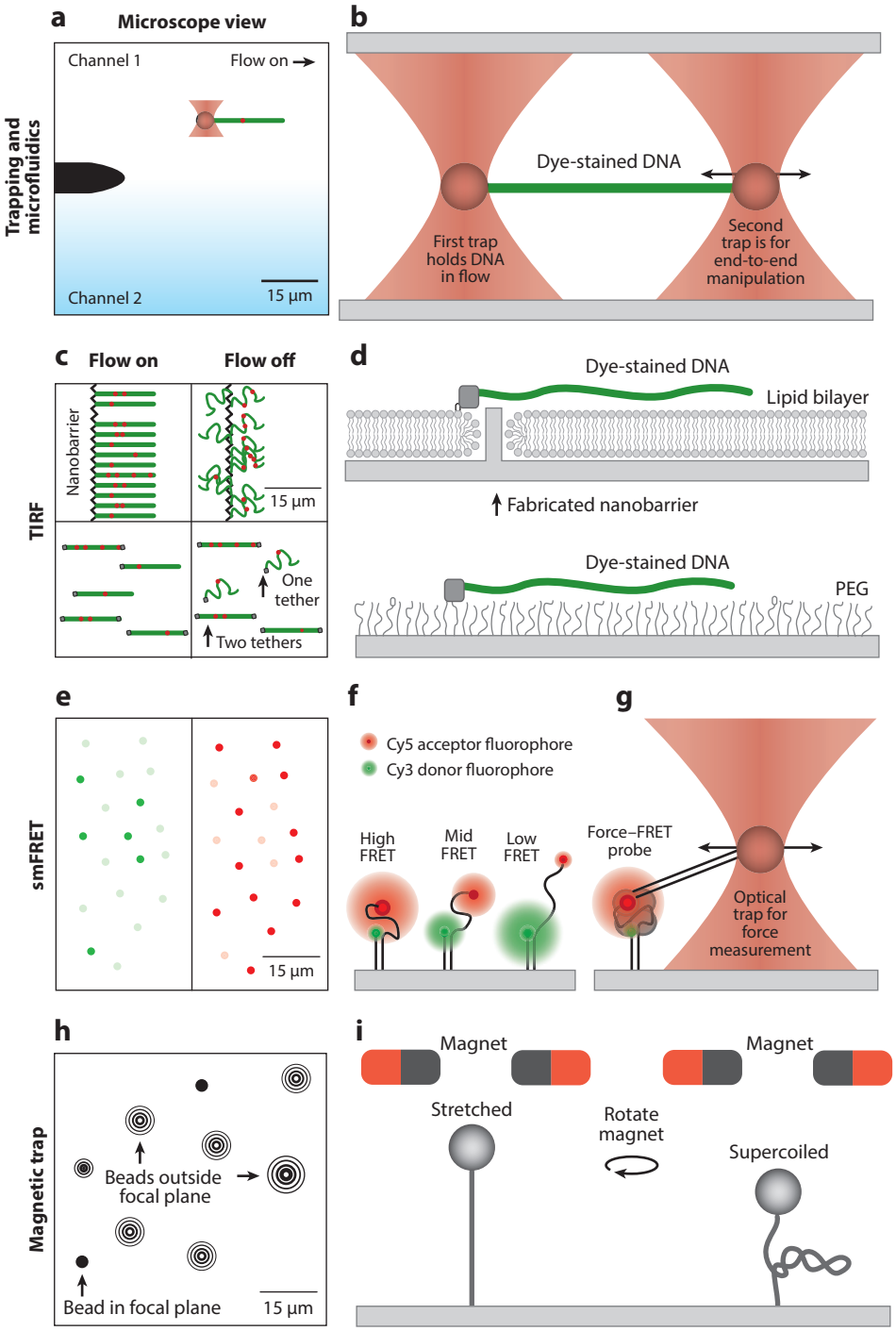

the bead's motion, measured with a sensitive quadrant photodiode, can be translated into force exerted on the molecule (35). In this way, force can be measured as a molecule is stretched. Alternatively, changes in DNA length (e.g., from DNA degradation, unwinding, or synthesis) can be measured at constant force. One especially powerful single-molecule method combines both force spectroscopy and fluorescence into a single experimental system, in which an optical trap can be used to manipulate a molecule containing a FRET dye pair tethered to a glass surface. In this way, the FRET pair is used to measure nanometer-scale changes in extension as force is applied by the optical trap (**Figure 2*g***) (36). Although the bead is often held in an optical trap in force spectroscopy experiments, another variation on this method uses a magnetic field to manipulate single molecules of DNA tethered to a glass surface on one end and a paramagnetic bead on the other: This is the so-called magnetic tweezers instrument (**Figure 2*h***) (37). Because the bead is sensitive to the polarity of the magnetic field, controlled rotation of the magnet can be used to rotate the bead to apply torque on the DNA, thus introducing or relaxing supercoils (**Figure 2*i***).

Recombination mediator: a class of proteins that promotes the formation of RecA or RAD51 filaments on SSB- or RPA-coated single-stranded DNA either by promoting filament nucleation and/or growth or by stabilizing filaments against disassembly

INITIATION OF RECOMBINATION BY RESECTION OF DNA ENDS IN *ESCHERICHIA COLI*

RecBCD Is a Master Regulator of Recombination from a DNA Break

In wild-type *E. coli*, the majority of double-strand breaks (DSBs) are processed by the multifunctional RecBCD enzyme, which has combined helicase, nuclease, and recombination mediator activities (38). The mechanism of RecBCD is both complex and elegant, requiring structural and single-molecule analysis to make full sense of many of its seemingly contradictory biochemical activities and genetic functions (**Figure 3*a***) (38, 39). The RecBCD holoenzyme binds to dsDNA

Figure 2

Single-molecule methods used to study DNA recombination. (*a*) Microscope view of an experimental system that uses one or more optical traps to manipulate single molecules of DNA, tethered to beads, within a microfluidic flow cell containing multiple channels that can be used to dip a DNA molecule into a solution containing protein, ligands, antibodies, etc. (*b*) Schematic of a dual optical trap used to manipulate the ends of a single molecule of DNA; flow is typically perpendicular to the DNA. (*c*) Microscope view of total internal reflection fluorescence (TIRF)-based visualization of protein (*red*)–DNA (*green*) complexes, shown with solution flow either on or off, using (*top*) lipid bilayer surfaces (*d*) that can be used to form an ordered array of DNA, a "curtain," resulting from flow that pushes the molecules tethered to biotinylated lipids via streptavidin either into a physical nanobarrier or (*bottom*, *c* and *d*) bound to a surface covalently coated with a biotinylated polymer [e.g., polyethylene glycol (PEG)], to which one or both ends of the DNA may be tethered. (*e*) Microscope view of a single-molecule Förster resonance energy transfer (smFRET) experiment in which the image is divided onto a single detector for fast, simultaneous imaging. (*f*) Schematic of a typical single-stranded DNA substrate depicting how the relative FRET changes as a function of distance between a donor fluorophore (Cy3) and an acceptor (Cy5). In the high FRET state, the Cy5 acceptor (*red*) is brightest, whereas the Cy3 donor fluorescence (*green*) is lowest owing to radiationless energy transfer. In the low FRET state, the intensities are opposite. (*g*) Molecules containing a FRET pair can be manipulated by tethering one end of the DNA to a bead in an optical trap for simultaneous fluorescence and force spectroscopy. (*h*) Microscope view of a surface to which magnetic beads are tethered. The Z position of each bead is measured based on the diffraction pattern of the bead as it moves away from the focal plane. (*i*) Schematic of a magnetic trap instrument: (*left*) When the magnet is moved closer to the bead, the force increases, stretching the molecule; (*right*) when the magnet is rotated, the twist of topologically constrained DNA changes, introducing or relaxing supercoils, which can cause the molecule to collapse and shorten.

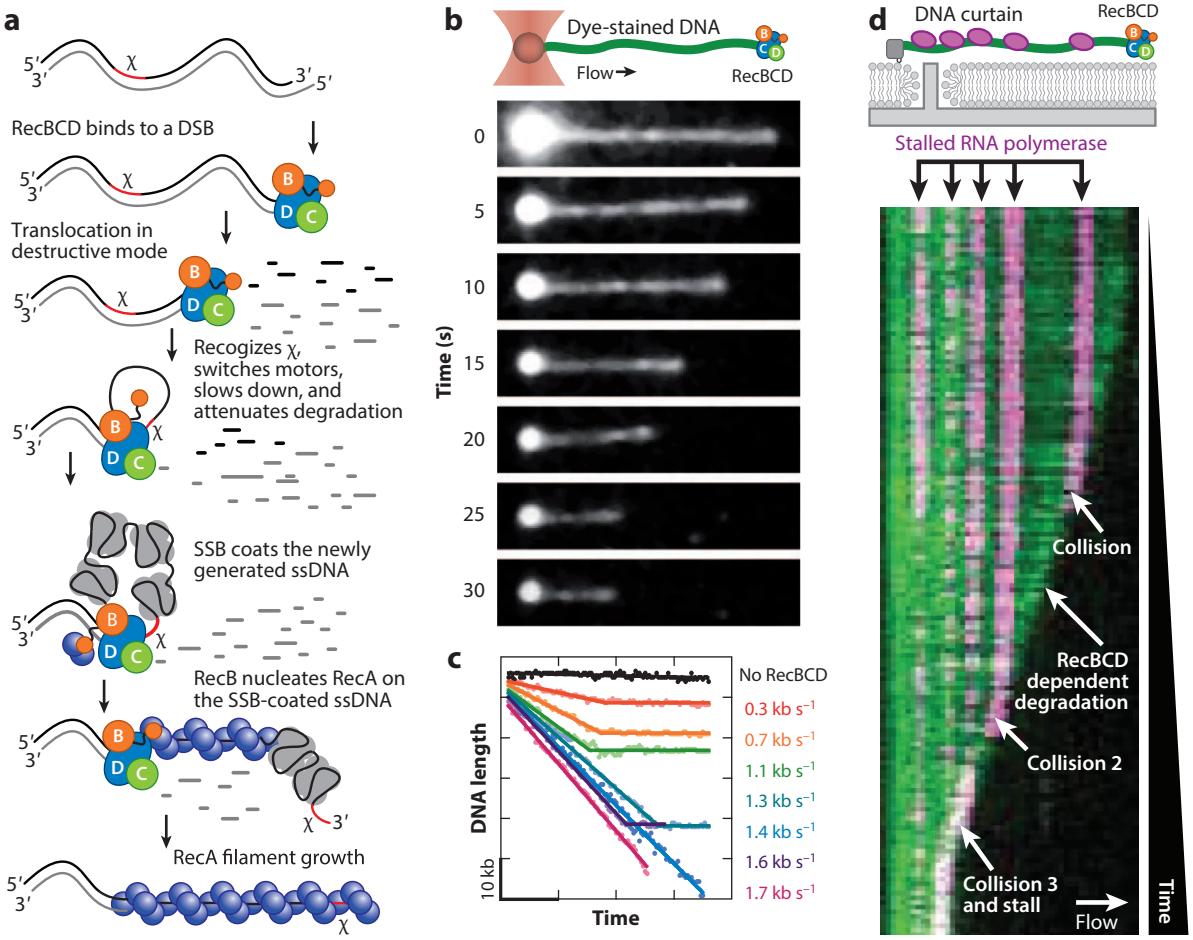

Figure 3

Initiation of recombination by DNA end resection in *Escherichia coli*. (*a*) RecBCD binds to a double-strand break (DSB) and resects the DNA through the coordinated action of two helicases and a nuclease, destroying both strands. When RecBCD encounters a self-recognition sequence, χ, distributed throughout the *E. coli* genome, it pauses, switches its lead motor, and alters its nuclease domain to protect the 3′-terminated strand, upon which it loads RecA to promote recombination. Gray tetramers represent single-stranded DNA (ssDNA)–binding protein (SSB). (*b*) Schematic and montage of a single molecule of DNA stained with YOYO-1 being processively degraded by RecBCD (not visible) (30). (*c*) Plot of DNA length versus time during RecBCD-dependent translocation and degradation, showing the intrinsic heterogeneity of translocation rates observed for different molecules of RecBCD (30). (*d*) Schematic (*top*) of a DNA molecule, visualized using total internal reflection fluorescence microscopy, tethered in a DNA curtain (see **Figure 2*c*,*d***). The image (*bottom*) is a kymograph, representing a single slice through the molecule projected through time, from top to bottom. DNA is YOYO-1–stained and extended by flow from left to right, and the pink spots are stalled RNA polymerase elongation complexes. The shortening on the DNA that occurs with time is due to RecBCD-dependent degradation and collision with the complexes (59). Panels *b* and *c* adapted from Reference 30, and panel *d* adapted from Reference 59, all with permission from Nature Publishing Group. Panel *b* adapted from Reference 170 with permission.

ends with a high affinity [dissociation constant (K_d) approximately 0.1–1 nM] and translocates while engaging both strands with each of its two motors, RecB, which is a 3′→5′ helicase, and RecD, a 5′→3′ helicase (40, 41). The net result is that the holoenzyme moves in the same direction along the dsDNA by simultaneously pulling on each of the strands, which are fed into separate channels (39). One of these channels is formed by the RecC subunit, which contains a

recognition motif that allosterically regulates the activity of the enzyme upon encountering the sequence designated χ (5′-GCTGGTGG-3′) (42–45). This sequence is called Chi (χ) because it is a crossover hotspot instigator (46).

RecBCD is the fastest known helicase, capable of unwinding DNA at an average rate of approximately 1,500 base pairs (bp) per second, although individual molecules have been clocked at up to 2,000 bp per second (30). The intrinsic asynchrony and heterogeneity in ensemble experiments made it difficult to ascertain how χ recognition altered the enzyme to promote recombination in ensemble measurements. These limitations were overcome by watching an individual RecBCD enzyme unwind and degrade a single molecule of bacteriophage lambda DNA (λ DNA, 48,502 bp) (28, 47). This was accomplished by attaching one end of the DNA—with RecBCD bound to the other free end—to a polystyrene bead held in an optical trap, and activating the enzyme by moving the molecule across a laminar flow boundary into a channel containing adenosine triphosphate (ATP) (28). The DNA was imaged using a fluorescent dsDNA intercalating stain, YOYO-1. In the presence of ATP, the enzyme translocates through the DNA from the end, unwinding and degrading both strands simultaneously (**Figure 3*b*** and **Supplemental Video 1.** To view all supplemental videos, access the article on the Annual Reviews website at **http://www.annualreviews.org.**). Two conclusions from these experiments were both obvious and surprising and could not have been discerned from traditional biochemical experiments. First, the enzyme degraded the DNA uniformly and unfalteringly until it reached its processive limit, around 30,000 bp. Second, although the rate of translocation for each RecBCD enzyme was uniform for a given molecule, when different molecules were compared the rates varied up to eightfold (28).

Before it recognizes χ, RecBCD functions in a destructive mode producing short oligonucleotide fragments owing to the combined helicase and nuclease activity, which is derived from the position of its nuclease domain at the exit point for both ssDNA channels (39). It had been well established that χ was a molecular switch that reduced DNA degradation by RecBCD (48, 49), but the enzyme was too fast and too asynchronous to ascertain the molecular details. By inserting the χ sequence into λ DNA, single-molecule experiments revealed that RecBCD pauses for 4–5 seconds at χ, after which translocation begins again, albeit at a slower rate (47). This pause is coupled to a conformational change in the enzyme that occurs upon χ recognition (44, 45). Because the rate after χ is identical to the rate of the enzyme when the RecD helicase is inactive, the slower translocation is attributed to the switching of the lead motor from RecD to RecB, but not to loss of the RecD subunit itself (50–53) (**Supplemental Video 2**). The RecB nuclease domain is also released from the enzyme, altering its activity so that the 5′-terminated strand is degraded and the 3′-terminated strand is protected (54). χ recognition also reveals a cryptic RecA loading activity that is essential for promoting homologous recombination (**Figure 3*a***) (55–57), which is attributed to a buried RecA binding surface on RecB that is revealed only after χ recognition and the subsequent release of the RecB nuclease domain (57). This binding surface facilitates the loading of RecA on the 3′-terminated ssDNA tail, relieving the kinetic inhibition by ssDNA-binding protein (SSB) (57). In this way, RecBCD serves an essential role in protecting the bacterium from invading DNA, as well as in promoting the repair of its own genome by degrading foreign DNA into small fragments (38), a property that some bacteria have co-opted as part of their CRISPR/Cas immune system (58) (see sidebar, The Role of RecBCD in CRISPR Adaptation).

Liu et al. (30) revisited the subject of the heterogeneity of RecBCD translocation rates (**Figure 3*c*** and **Supplemental Video 3**), asking whether the nature of this heterogeneity was dynamic or static. In other words, they asked whether a single enzyme could adopt multiple states that define its biochemical activity for an experimental lifetime (i.e., dynamic heterogeneity) or whether each enzyme has a single invariant state (i.e., static heterogeneity). To address this question, they first attempted to thermally and chemically refold RecBCD into a homogenous

THE ROLE OF RecBCD IN CRISPR ADAPTATION

Recently, it was discovered that the products of RecBCD-dependent DNA degradation are the source for the sequences acquired by the clustered regularly interspaced short palindromic repeat (CRISPR) system, an adaptive immune system in bacteria that protects against bacteriophage infection and plasmid transformation (58). Levy et al. (58) mapped the acquisition of new foreign DNA (i.e., protospacers) into an artificial and naive CRISPR array during adaptation. They found that protospacer acquisition was strongly correlated with regions prone to replication-fork stalling and thus were susceptible to forming spontaneous dsDNA breaks. Strikingly, protospacers were distributed across the entire genome but were diminished when flanked by properly oriented χ sequences, prompting the authors to ask whether RecBCD plays a role in adaptive immunity. Indeed, deletion of *recB*, *recC*, or *recD* led to a marked reduction in new protospacer acquisition. Notably, the CRISPR system exhibits a strong preference for the acquisition of foreign DNA lacking χ because the pre-χ mode of RecBCD degradation produces the short oligonucleotide fragments recognized via Cas2, which binds the DNA fragments. In contrast, the "self" *Escherichia coli* chromosome contains an overrepresentation of χ sequences (1 per ∼5 kbp), and DNA after χ sites is not degraded. Consequently, the host DNA is statistically "immune" from the CRISPR system.

population based on the hypothesis that static heterogeneity could be attributed to subpopulations of enzymes that were kinetically trapped as folding intermediates. Surprisingly, neither of these attempts produced a more homogenous population. They then asked whether the heterogeneity could be attributed to a kinetically stable conformational state defined by ligand binding (i.e., Mg^{2+}:ATP) by interrogating the consequence of depleting the ligand from an actively translocating molecule of RecBCD and then reactivating it. Ligand depletion halted translocation, and when the molecule was reactivated with Mg^{2+}:ATP, approximately half of the molecules resumed (the other half presumably dissociated). Of the molecules that resumed translocation, half resumed at their previous rate, whereas one-third slowed down and the remainder sped up. This new distribution of rates (i.e., after depletion and rebinding) recapitulated the original distribution of the entire population preceding ligand depletion. Therefore, each RecBCD enzyme is capable of switching into microstates that define its biochemical properties, but each microstate can be maintained for an unusually long lifetime. This observation is consistent with the ergodic hypothesis, which posits that the infinite, time-averaged behavior of a single molecule at equilibrium is equal to the ensemble average of an infinite collection of those molecules (30).

In each of these experiments, the degradation of DNA by RecBCD was assayed on naked DNA; however, in the context of the cell, RecBCD is expected to collide with DNA-bound proteins, including transcription factors and actively transcribing RNA polymerase (RNAP). Using arrays of DNA curtains, molecular obstacles—including RNAP, stalled and active elongation complexes of RNAP, lac repressor, catalytically inactive endonucleases ($EcoRI^{E111Q}$), and even nucleosomes—were preassembled on DNA and challenged with RecBCD (59). When RecBCD collided with the RNAP elongation complexes, most were pushed, though a small number of obstacles were ejected or caused RecBCD to stall (**Figure 3*d***). Similar results were obtained when $EcoRI^{E111Q}$ was used; however, lac repressor was almost invariably ejected at each collision. When RecBCD collided with an obstacle that it continued to push, its velocity remained unchanged, except in the special case of the nucleosome, which induced a 10% reduction in speed (59, 60).

RecQ Initiates Unwinding Through Duplex DNA Melting Followed by Bubble Expansion and Coordinates with RecJ for Resection of Stalled Replication Forks

Replication-associated breaks can be blunt, tailed, or gapped, depending on the strand that is nicked and whether the replisome collapses or continues with uncoupled synthesis. These broken molecules are repaired by the RecBCD and RecFOR pathways, distributed, respectively, approximately 60% and 40% (61, 62). Importantly, RecBCD requires a nearly blunt DNA end to initiate unwinding and degradation and is blocked by long ssDNA overhangs (38). In the RecFOR pathway, recombination is initiated by RecQ, a 3′→5′ helicase, and RecJ, a 5′→3′ exonuclease, which provide complementary functions to process and resect all types of dsDNA ends: 5′-overhangs, blunt, or 3′-overhangs (63). RecQ is nearly unique in its ability to initiate unwinding on any DNA substrate, requiring neither an end nor ssDNA; however, at physiological concentrations of Mg^{2+}, RecQ is an inefficient helicase (64). Its helicase activity is stimulated by SSB in a distinctive manner: SSB traps the kinetic products of unwinding, competitively prevents product-inhibition of RecQ by binding to the ssDNA produced, which otherwise sequesters the RecQ; it also stimulates the elongation, but not the initiation, of unwinding through a direct interaction with RecQ via the C-terminal tail of SSB (63, 65). In the absence of SSB, the processivity of RecQ translocation on ssDNA is only 20–40 nucleotides (nt) (66, 67). Recently, Rad et al. (68) used fluorescently modified SSB and TIRF microscopy to directly visualize RecQ helicase activity on single molecules of dsDNA tethered at each end to a glass surface. When the molecules were incubated with RecQ, Mg^{2+}:ATP, and fluorescent SSB, long tracts of SSB formed, coinciding with the formation of ssDNA bubbles or, alternatively, dimmer tracts with a bright spot at one or both ends, coinciding with fork movement where one unwound strand was nicked and collapsed around the fork (**Supplemental Video 4**) (68). By measuring the migration of the forks and the length of each fluorescent SSB tract, both the rate and processivity of RecQ molecules could be ascertained. When free RecQ was washed out of the flow cell, SSB tracts continued to grow, demonstrating that individual complexes of RecQ could translocate, on average, 1,000–2,000 nt at approximately 40–60 nt/s. Finally, the apparent cooperativity of RecQ, measured by both stopped-flow kinetics and single-molecule visualization, led to the proposal that a dimer of RecQ is optimal for initiation of DNA unwinding through duplex melting. The initiation by dimers also explained the observation that approximately 25% of unwinding tracts grew bidirectionally; it is unknown whether the unidirectional forks are from initiation by monomers or from bidirectional nucleation events in which one of the forks either failed to propagate or dissociated. Rad et al. (68) also proposed that the elongation of unwinding proceeds though dynamically assembled, variable-sized multimers (4–6 monomers) that travel at a distribution of speeds proportional to their size, a mechanism to "fine tune" DNA fork movement (69).

INITIATION OF RECOMBINATION AND DNA END RESECTION IN EUKARYOTES

Processing of Double-Strand Breaks in Eukaryotes: Competitive Collaboration Among Mre11–Rad50–Xrs2, Sgs1–Dna2, and Exo1

Similar to the complementary ways in which RecBCD, RecQ, and RecJ have overlapping mechanisms to initiate DNA end resection in bacteria, eukaryotes have several alternative pathways by which DNA ends may be processed (70). Shortly after a dsDNA break occurs, the

heterotrimeric complex Mre11–Rad50–Xrs2 (MRX) binds to a DSB. In vitro, MRX possesses a 3′→5′ exonuclease activity that is the opposite to what is conventionally expected for HR, puzzling biochemists and geneticists for years. An experimental resolution of this complex issue was recently and elegantly provided by Cannavo & Cejka (71), who demonstrated that MRX has an intrinsic and cryptic endonuclease activity that is activated by binding to Sae2, nicking the DNA approximately 15–20 nts proximal to a break and then using its 3′→5′ exonuclease activity to produce a short, 3′-terminated ssDNA tail.

The short-range resection by MRX (MRN in humans) produces an important intermediate that commits a DSB to HR versus nonhomologous end joining (NHEJ), at which this commitment coincides with extension of the resected end to produce a long ssDNA region upon which a Rad51 filament forms (70). This long-range resection proceeds through two alternative routes: the Sgs1/Dna2 pathway and the Exo1 pathway (70). Sgs1 is the only RecQ helicase in *Saccharomyces cerevisiae* and is the homolog of human BLM helicase. Sgs1 has a 5′→3′ unwinding directionality that is greatly stimulated by yeast RPA (replication protein A) (72) and forms as a stable complex with topoisomerase 3 (Top3) and Rmi1, commonly called the STR complex (6). Dna2 (DNA2 in humans) is a potent nuclease that degrades ssDNA in both the 5′→3′ and 3′→5′ directions (73); however, RPA inhibits the 3′→5′ activity and stimulates the 5′→3′ activity, thereby imposing a strict degradation polarity in the 5′→3′ direction (74, 75). Though different in detail and arising from divergent protein families, the Sgs1–Dna2–RPA complex is the functional analog of χ-modified RecBCD in the context of long-range DNA end resection.

Using magnetic tweezers to measure the unwinding activity of single-molecules of Dna2, Levikova et al. showed that when the nuclease function is inactivated, Dna2 is a vigorous 5′→3′ helicase, unwinding at variable rates ranging from 15–120 bp/s and translocating approximately 4 kb per unwinding event. This helicase activity manifests only when the nuclease is made nonfunctional because, ironically, the native nuclease activity degrades the ssDNA in front of the motor domain (76). In other words, the enzyme seemingly pointlessly destroys the track on which it moves—much like someone sawing off the limb of a tree on which they are working—and therefore immediately falls off the DNA. In the context of resection, this action is of little consequence because Dna2 is associated with Sgs1, which functions as the 3′→5′ motor while Dna2 engages and degrades the 5′-terminated strand repeatedly (74, 75). Therefore, the Sgs1–Dna2 complex functionally resembles RecBCD after χ recognition insomuch as the complex is composed of two motors with opposite translocation polarities coupled to an endonuclease that degrades the 5′-terminated strand and functions in a concerted way to produce a 3′-terminated ssDNA tail (74). It is worth noting that Sgs1 is a multifunctional enzyme that, when in complex with Rmi1 and Top3, also plays an important role in the migration and dissolution of Holliday junctions (6).

The alternative mechanism for the resection of dsDNA is via Exo1 (EXO1 in humans), a 5′→3′ XPD-family exonuclease (77–79). Similar to observations made for Sgs1–Dna2, the MRX complex stimulates resection by recruiting Exo1 to the DNA ends (77, 80). RPA also stimulates Exo1 and confers specificity to the dsDNA–ssDNA junctions by stimulating the resection of dsDNA but blocking exonucleolytic degradation of RPA-coated ssDNA (77). In other words, in *S. cerevisiae*, once Exo1 is recruited to a DNA end or junction (i.e., at a gap or tail), RPA stimulates resection by enforcing productive processive degradation to produce a 3′-terminated ssDNA tail or overhang; however, RPA blocks initiation of Exo1 degradation of 5′-terminated ssDNA tails. This inhibition of Exo1 by RPA supports the interpretation that not only are the Sgs1/Dna2 and Exo1 resection pathways independent but they are also mutually exclusive, owing to the fact that Exo1 cannot degrade the RPA-coated ssDNA products of Sgs1 unwinding (77).

THE ROLE OF SINGLE-STRANDED DNA BINDING PROTEINS IN RECOMBINATION

SSB Cooperatively Slides, Wraps, and Jumps Across ssDNA to Melt Secondary Structure and Protect ssDNA

E. coli SSB binds to ssDNA rapidly and with a high affinity (81). Each tetramer of SSB wraps ssDNA around itself and has a variable site size, which reflects either a fully wrapped or partially wrapped state (82). SSB functions to exclude access to ssDNA, protecting it from nucleases, and creates a kinetic barrier that prevents the assembly of RecA filaments on Okazaki fragments during DNA replication. Despite this inhibitory role, SSB also stimulates RecA-mediated recombination by denaturing secondary structure that otherwise impedes the formation of RecA filaments (83). When ssDNA is fully wrapped around an SSB tetramer, the two ends are brought into close proximity, making single-molecule FRET an exceptionally powerful method for measuring the dynamics of SSB on ssDNA (22, 33). In such experiments, a short oligonucleotide pair is labeled with a donor fluorophore at one end (usually at a dsDNA–ssDNA junction) and an acceptor fluorophore at the distal end of an ssDNA overhang (33) (see, e.g., **Figure 2*g***). The time-dependent fluctuations between these states under various biochemical conditions report on the binding, wrapping, and sliding of SSB to ssDNA (84, 85). SSB is seen to rapidly and transiently melt the secondary structure in this assay; the melting results from SSB diffusively sliding into the hairpin during DNA breathing. In an extension of this approach, Zhou et al. (36) used a particularly sophisticated single-molecule method that combines both force and fluorescence spectroscopy to measure SSB sliding on ssDNA using an optical trap to stretch the ssDNA between two FRET reporters (**Figure 2*g***). This system was used to measure the force required to dissociate a single SSB tetramer (approximately 6–12 pN) (36), as well as the diffusion of SSB on long (approximately 10,000 nt), otherwise bare, ssDNA substrates, providing evidence that SSB undergoes rapid, intersegmental transfer by engaging ssDNA sites separated by long distances along the ssDNA backbone but that are close in the context of a collapsed polymer (86–88). In agreement with these observations, SSB-coated ssDNA undergoes reversible intramolecular condensation in response to small perturbations in solution conditions that alter the wrapping state of the ssDNA around the tetramer (**Supplemental Videos 5 and 6**). These changes enable SSB to engage either other tetramers or distant sites along the ssDNA and are modulated by the SSB-interacting and recombination mediator proteins RecOR (see section on "RecFOR and RecOR Accelerate Nucleation and Growth of RecA on SSB-Coated Single-Stranded DNA") (88).

RPA Slides, Jumps, and Melts, but Does Not Wrap

RPA is the eukaryotic homolog of SSB, is highly conserved among eukaryotes, and has pleiotropic functions during replication, recombination, and DNA repair (89, 90). At the structural level, although the ssDNA-binding domains (the so-called oligonucleotide-binding folds) are similar, *E. coli* SSB and human RPA bear no overall resemblance to each other, despite their conservation of function (91, 92). Similar to experiments performed with SSB, single-molecule experiments have demonstrated that RPA slides (5,000 nt^2/s at 37°C) on ssDNA and melts secondary structure (93). RPA remains stably bound to ssDNA for long lifetimes (on the order of tens of minutes to hours) in the absence of free protein in solution, but when challenged with RPA labeled with a different fluorophore, RPA can be rapidly exchanged on single molecules of ssDNA (94). In this regard, the behavior of both *E. coli* SSB and RPA is similar (95, 96), owing to the multiple ssDNA-binding sites on each protomer (97). The long lifetimes in the absence of free protein is due to the multiple binding surfaces simultaneously interacting with the ssDNA in an uncoordinated

fashion, so that the net probability of dissociation is low in the absence of a competitor protein (i.e., free RPA or SSB associating in *trans*).

RECOMBINATION MEDIATORS OVERCOME MOLECULAR COMPETITION

Nucleation and Growth of RecA on Single Molecules of DNA

The catalyst for DNA pairing and strand exchange in bacteria is the RecA filament: the mechanical and molecular core of homologous recombination (see 98). To function, RecA must form a filament on the ssDNA, but it is kinetically blocked from binding by the rapid and contiguous association of SSB to suppress unwanted recombination (96, 99, 100).

Filament-forming proteins assemble in two phases: nucleation followed by growth. Although methods for measuring these parameters for proteins, such as actin and tubulin, have existed for decades (101, 102), the complexity of forming a filament on a linear template in the presence of a contiguous kinetic competitor precluded these measurements for RecA using traditional biochemical methods. A major advance was to use optical trapping to capture a single dsDNA molecule and iteratively dip the molecule into a solution containing fluorescently labeled RecA (**Figure 4*a***), which was then imaged to directly measure nucleation and growth (**Figure 4*b***) (29). At the same time, single-molecule FRET was used to measure the nucleation and growth of RecA on short ssDNA molecules with remarkable precision, measuring the on-rate and off-rate of individual RecA monomers (**Figure 4*c***) (103). Although the displacement of SSB could be observed from filaments preformed before adding SSB (**Figure 4*d***), the potent kinetic competition imposed by SSB precluded the measurement of RecA nucleation on SSB-coated ssDNA (103).

To measure the formation of RecA filaments in the presence of SSB, TIRF microscopy was used to directly image nascent filaments on individual molecules of SSB-coated ssDNA—the natural in vivo substrate for RecA (**Figure 4*e*** and **Supplemental Video 7**) (96). These experiments first visualized SSB-coated ssDNA, then exchanged the fluorescently labeled SSB with wild-type, unlabeled SSB. When RecA was then added, clusters of RecA formed on the SSB-coated ssDNA, and these clusters grew linearly with time in both length and intensity. Two parameters were extracted from these experiments: the nucleation frequency, determined by the number of new clusters formed with time, and the growth rate, determined by the time-dependent length increase (96). By analyzing the kinetic relationship between nucleation and RecA concentration, the critical nucleus was found to be a RecA dimer, corresponding to a site size of six nucleotides (roughly 1/10 the footprint of SSB). Single-molecule FRET experiments had demonstrated that SSB is highly dynamic: sliding, wrapping, and jumping between distant sites (36, 84, 85). Owing to this mobility of SSB on ssDNA, RecA could form a spontaneous nucleus only during the rare event when SSB transiently dissociated from an ssDNA segment—through sliding, unwrapping, or dissociating—and when a dimer of RecA could diffusionally collide with, or sequentially assemble on, the transiently free ssDNA. The growth of filaments occurred linearly from both ends, albeit with twofold faster growth in the 5′→3′ direction, and both the concentration and nucleotide-ligand dependence suggested that growth proceeded through monomer addition (96).

RecFOR and RecOR Accelerate Nucleation and Growth of RecA on SSB-Coated ssDNA

In vivo, the assembly of RecA filaments must be tightly regulated to prevent unwanted recombination, particularly in the context of a replication fork, where the formation of a RecA filament

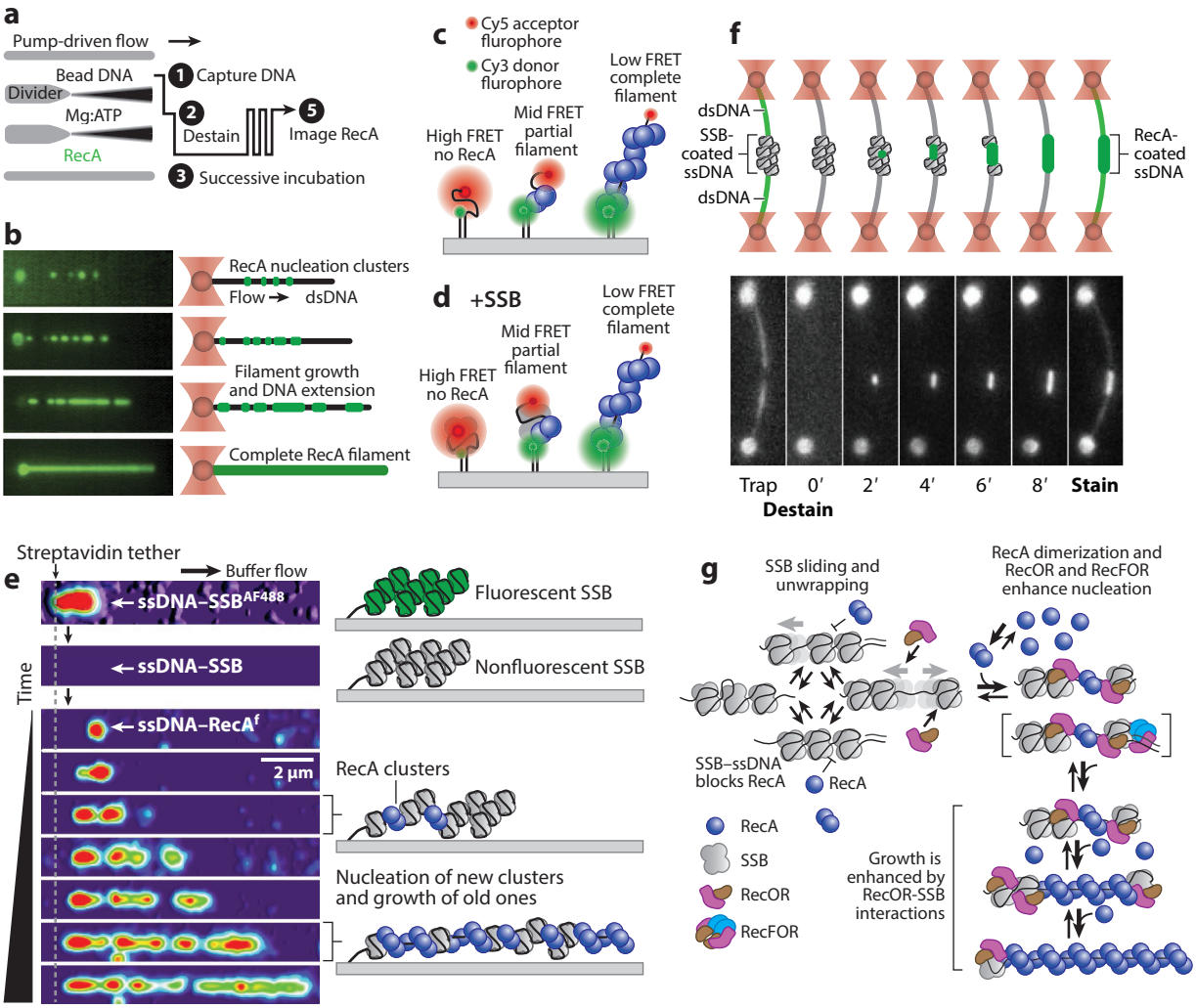

Figure 4

Presynaptic filament formation: RecA and RecFOR. (*a*) Schematic depicting an optical trap and microfluidic configuration used to dip a molecule of double-stranded DNA (dsDNA) into a solution of fluorescent RecA followed by (*b*) successive imaging of the molecule (*montage*) to measure filament nucleation and growth. (*c*) Schematic of single-molecule Förster resonance energy transfer (FRET) experiments used to measure RecA filament dynamics on single-stranded DNA (ssDNA) alone or (*d*) with ssDNA-binding protein (SSB). (*e*) Montage of a single molecule of fluorescent SSB-coated ssDNA (*top*) before and after exchange with unlabeled SSB, followed by a time course monitoring fluorescent RecA nucleation and growth on the SSB-coated ssDNA. The fluorescence intensity along the molecule is represented as a heat map, with red as the brightest and purple as background. (96). (*f*) (*top*) Schematic and (*bottom*) images of RecA filament assembly on an ssDNA region integrated into λ DNA used to measure the contribution of RecF and RecOR to the assembly of RecA filaments; in the first and last images, the dsDNA is stained with YOYO-1 (96). (*g*) Model depicting the kinetic inhibition imposed by SSB to block spontaneous nucleation of RecA dimers, which is overcome by RecOR- or RecFOR-dependent binding to the SSB-coated ssDNA. RecOR, but not RecF, binding to the SSB-coated ssDNA enhances the growth rate of RecA (96). Panels *a* and *b* adapted from References 29 and 171 with permission from Elsevier. Panels *e–g* adapted from Reference 96 with permission from Nature Publishing Group.

on the lagging strand could impede replication or inadvertently activate the SOS response. The kinetic inhibition imposed by SSB is the primary mechanism by which RecA filament formation is suppressed, and this inhibition is overcome by recombination mediator proteins (99, 104, 105). In *E. coli*, these recombination mediator proteins are RecF, RecO, and RecR (99), which form two functional subcomplexes, RecOR and RecFOR. RecOR binds SSB, while the RecFOR complex binds at the 5′-end of a junction between dsDNA (or an RNA–DNA duplex) and ssDNA, with an affinity of approximately 1–2 n*M* and a specificity of 1,000-fold over ssDNA (104, 106). In doing so, RecFOR recruits RecA to nucleate at that junction within minutes; this nucleated filament can grow during the course of 10–15 minutes to approximately 1,000–2,000 nt in the 5′→3′ direction from the junction.

To produce a gapped DNA substrate suitable to assay RecOR and RecFOR functions, a circular ssDNA was site-specifically integrated into λ phage DNA (96). This gapped DNA molecule was then tethered between two optically trapped beads and dipped into channels containing RecA, with or without mediator proteins (**Figure 4*f*** and **Supplemental Video 8**). The addition of RecOR shifted the distribution to shorter lag times, stimulating nucleation approximately twofold. Similarly, the average growth rate in the presence of RecOR was threefold faster. With RecFOR, nucleation—but not growth—was further stimulated, consistent with its role as a structure-specific nucleation factor at the dsDNA–ssDNA junction (**Figure 4*g***). Together, the RecFOR proteins stimulated RecA filament formation approximately 10-fold, and some filaments completely formed on the entire ssDNA gap (approximately 8,200 nt) in the time typically required for RecA alone to form a single nucleus (96). Minimally, one might expect that nucleation of a RecA filament should be several-fold slower than the lifetime of an ssDNA gap resulting from lagging strand synthesis, which is an ideal substrate for RecFOR-stimulated RecA filament formation, but it is filled on the order of a few seconds (106). Indeed, even when stimulated by RecFOR, RecA filament nucleation requires minutes, consistent with a built-in kinetic delay to recognize stalled replication forks, and is clearly much faster than the spontaneous rate of RecA nucleation that approaches or exceeds the doubling time of *E. coli* (96).

Rad52 and the Rad51 Paralogs Promote Rad51 Filament Nucleation

Analogously, for a RAD51 filament to form, it too must overcome the kinetic inhibition imposed by RPA (107). In *S. cerevisiae*, the functional homolog of RecO is Rad52, which forms a heptameric ring in solution, anneals RPA-coated ssDNA, and stimulates Rad51 filament formation by directly binding to both RPA and Rad51, thus functioning as a molecular bridge (107–110). Recent single-molecule imaging of Rad52 binding to RPA-coated ssDNA revealed an interesting, and previously unknown, phenomenon: Rad52-bound RPA was stabilized, preventing exchange with free RPA in solution. Gibb et al. (111) directly visualized this stabilization by binding fluorescent Rad52 to ssDNA coated with RPA-mCherry and then replacing the solution with unlabeled RPA, observing RPA exchange only in regions where Rad52 was absent. A second previously unknown phenomenon was that Rad52 binds to RPA-coated ssDNA cooperatively, exhibiting concentration-dependent nucleation and growth of these cooperative assemblies (**Figure 5*a***) (111). Although it had long been established that Rad52 promotes Rad51 filament formation on RPA-coated ssDNA, many of the intermediate steps were unknown (107–110). To address these issues, Gibb et al. (111) co-visualized RPA and Rad52 during Rad51 filament formation, with the expectation that the disappearance of fluorescence would coincide with the Rad51-mediated displacement of each protein. Surprisingly, but consistent with their observations in the RPA exchange experiments, Rad52 stabilized the RPA to which it was bound (**Figure 5*b***), while promoting Rad51 nucleation on adjacent, RPA-coated ssDNA (**Figure 5*c***).

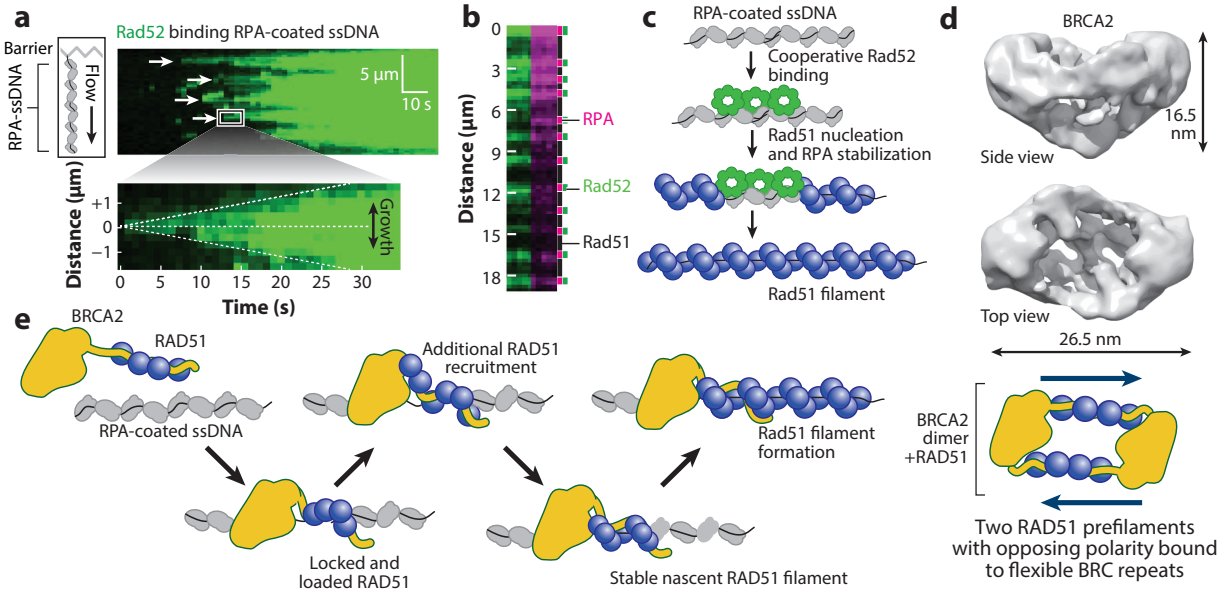

Figure 5

Presynaptic filament formation: Rad51, Rad52, and BRCA2. (*a*) The schematic (*left top*) and kymograph depict cooperative binding of Rad52 to RPA (replication protein A)-coated single-stranded DNA (ssDNA), demonstrating typical features of nucleation (*white arrows*) and growth (*bottom*, zoomed-in feature from kymograph). (*b*) Image of a single molecule after Rad51 (unlabeled, *black*) filament assembly on RPA-coated ssDNA (*magenta*) in the presence of Rad52 (*green*), showing stabilization of preexisting RPA by Rad52. (*c*) Model of Rad52-dependent stabilization of RPA and assembly of a Rad51 filament. (*d*) Model of BRCA2-dependent nucleation of RAD51 onto RPA-coated ssDNA. (*e*) Three-dimensional reconstruction of the BRCA2–RAD51 complex depicting a (*left*) side and (*center*) top view, and (*right*) a cartoon schematic showing the opposing polarity of the bound pre-nucleated RAD51 (128). Panels *a* and *b* adapted from Reference 111 and panel *e* adapted from Reference 128, all with permission from Nature Publishing Group.

S. cerevisiae also has several Rad51 paralogs: Rad55 and Rad57, which form a heterodimer and have primary sequence homology to the RecA/Rad51 core domain, and also Psy3-Csm2, which are part of the heterotetrameric Shu complex (Shu1–Shu2–Psy3–Csm2) (112). Mutations in Rad55 or Rad57 are sensitive to DNA-damaging agents; however, this sensitivity can be suppressed by overexpressing Rad51, by expressing a Rad51 mutant with an enhanced ability to form filaments, or by mutating Srs2, a helicase and anti-recombinase that disrupts Rad51 filaments (113, 114). These observations parallel the suppressor behavior seen in *recF*, *recO*, and *recR* mutants, and suggest that the Rad51 paralogs function to either stimulate Rad51 filament formation or to stabilize filaments against disassembly. Indeed, Rad55-Rad57 has been shown biochemically to bind to Rad51 filaments and protect them from disruption by Srs2 (115). The Shu proteins have been more recently identified in a genetic screen, owing to their suppression of the slow-growth phenotype in *top3*Δ cells, and then recognized to share a phenotype with *rad55* and *rad57* (116, 117). The Shu proteins bear little or no sequence homology to Rad51 or to other Rad51 paralogs; however, Psy3-Csm2 structurally mimics a dimer of Rad51 (112). The Shu complex binds to and stabilizes Rad51 filaments in a nucleotide-independent manner, presumably through this structural mimicry, but by an unknown mechanism (112). Recently, the ability of the Rad51 paralogs—alone and in combination with Rad52—to stimulate Rad51 filament formation on RPA-coated ssDNA was tested under conditions in which stimulation from Rad52 was limiting (118). When either Rad55–Rad57 or the Shu complex was incubated with Rad51 and RPA-coated ssDNA,

Gaines et al. (118) observed, respectively, only a very slight increase or no increase in filament formation. However, when the proteins were combined—specifically in the presence of Rad52—a greater than additive stimulation of Rad51 filament formation was observed (118).

BRCA2: A Chaperone for RAD51

The primary means by which nascent human RAD51 filaments are formed on RPA-coated ssDNA is through deposition by *BRCA2*, one of two familial breast cancer-susceptibility genes (119, 120). In contrast with yeast, human RAD52 cannot stimulate RAD51 filament formation in vitro, but it retains its capacity to anneal ssDNA coated with human RPA (119). BRCA2 is a very large protein (390 kDa) that chaperones RAD51 to RPA-coated ssDNA via its DNA-binding domain, which has three oligonucleotide-binding folds and an array of RAD51-binding motifs called the BRC repeats (121, 122). All *BRCA2* homologs have these two essential features, although the number of BRC repeats is highly divergent; there are eight in humans and mice, six in chicken, four in *Arabidopsis*, and one in *Caenorhabditis elegans* (122). The purified full-length human BRCA2 protein binds at least six molecules of RAD51, but neither RPA nor RAD52; it binds approximately four of these RAD51 molecules with a high affinity (K_d approximately 1 nM), and two or more with much lower affinity. As expected, it also binds ssDNA with high affinity (K_d approximately 1 nM), and does so without showing much (< twofold) junction-specific preferences. Unexpectedly, BRCA2 inhibits ATP hydrolysis by RAD51, but this has the favorable consequence of stabilizing the RAD51-ssDNA nucleus or nascent filament. Finally, by virtue of these combined effects, BRCA2 promotes the assembly of RAD51 on ssDNA that is occluded by RPA and stimulates DNA strand exchange (119). Because RAD51, like RecA (29, 96), can grow bidirectionally (123), the loading of RAD51 anywhere on ssDNA would allow the RAD51 filament to grow in either direction on the filament, although this may require multiple nucleation events on long stretches of ssDNA. Offering insight into BRCA2 function, the purified BRC repeat peptides affect RAD51 filament assembly and DNA pairing function, and they fall into two distinct classes (124–127). In one class—composed of BRC-1, -2, -3, and -4—each peptide binds to free RAD51 with high affinity, blocks ssDNA-dependent ATP hydrolysis, and prevents aberrant binding of RAD51 to dsDNA. In the other class—composed of BRC-5, -6, -7, and -8—each binds to RAD51 after it has formed a filament, and prevents its disassembly (125, 127).

Within the context of the full-length protein, these BRC repeats are presumably oriented in such a way as to build a preformed nucleation complex, where almost one helical turn of the filament is locked and the other turn is loaded when BRCA2 chaperones RAD51 to ssDNA (119, 125, 127). Indeed, three-dimensional (3D) electron microscopy reconstruction of BRCA2 alone and the Rad51-bound complex shows that BRCA2 can form a dimer (**Figure 5*d***), in which each monomer preassembles a partial RAD51 filament consisting of four to five monomers (**Figure 5*e***) (128). BRCA2 oligomerization is compatible with single-molecule tracking and fluorescence-correlation spectroscopy of free BRCA2 in live cells (129). These prenucleation complexes are oriented in opposite directions from each other, eliciting a model in which BRCA2 deposits only one Rad51 cluster and either retains or releases the other (128). However, whether the functional form that binds to ssDNA is a monomer or dimer remains unclear. Recently, it was demonstrated that DSS1, a highly acidic protein that is 70 amino acids long, bridges BRCA2 and RPA, functioning as an ssDNA mimic (130). Whether additional BRCA2-interacting factors [e.g., PALB2 or the RAD51 paralogs (131)] differentially direct the protein to specific structures, such as a junction or a replication fork, remains to be determined. BRCA2 also mediates loading of human DMC1, the meiotic RAD51 ortholog, onto RPA-coated ssDNA by a mechanism that is similar to that used for RAD51 delivery but which uses a different subset of BRC repeats (132).

FINDING THE RIGHT TARGET: MECHANICS OF THE DNA HOMOLOGY SEARCH AND ITS RECOGNITION BY RECA AND RAD51

The Homology Search Uses Parallel Processing to Reduce Dimensionality

Intersegmental contact sampling: the parallel processing mechanism by which RecA or RAD51 filaments assembled on single-stranded DNA engage in multiple contacts with double-stranded DNA during the homology search

Once a RecA filament has formed on a damaged chromosome, it must use the sequence information from the ssDNA within the nucleoprotein filament to find a homologous region and then exchange the individual strands needed for downstream template-directed DNA repair steps. The use of a DNA template to which a protein is bound to define a highly adaptable, sequence-specific targeting mechanism is an unusual but essential process that must be tightly regulated to prevent undesirable and potentially deleterious recombination. It is analogous only to the recently discovered class of proteins called CRISPRs (clustered regularly interspaced short palindromic repeats), which use RNA instead of DNA as the target guide (133). RecA filament formation requires the binding of ATP, which acts as a conformational effector that modulates the relative stability of the filament (134). The RecA filament mechanically stretches the ssDNA upon which it forms by approximately 150–160% (relative to an equivalent and corresponding length of B-form dsDNA), a process that is strictly required for RecA to pair the target ssDNA with homologous dsDNA. The failure of RecA mutants to adopt the high-affinity, stretched ssDNA filament conformation is the strongest morphological factor correlating with lost or reduced function (135).

The stretched ssDNA within the nucleoprotein filament adopts an unusual conformation that was surprising and unpredicted before the crystal-structure of the ssDNA–RecA complex was solved (136). Rather than being stretched isotropically, RecA holds the ssDNA in short, B-form triplets separated by a 7–8 Å gap. By using ATP-binding as a conformational effector to stretch both forms of DNA in the filament, RecA employs credit-card energetics—that is, the energy required for DNA strand exchange is coupled to filament disassembly, well after the kinetic steps of pairing and exchange are complete (134, 137). Although the molecular details of the energetics of DNA strand exchange were greatly informed by structural biology, the kinetic mechanism by which RecA uses the ssDNA within the nucleoprotein filament to search for homology remained elusive. Unlike site-specific DNA-binding proteins, such as transcription factors (e.g., lac repressor), RecA does not have a fixed sequence-specific binding site that can be hardwired using a protein motif. Rather, it must sense whether the paired DNA is a match through canonical or noncanonical base pair recognition with the filament, which it can detect only after binding and transiently stretching the potential target dsDNA in its secondary site to determine whether it is homologous (138). Furthermore, it must do this rapidly and efficiently, given the vast excess of heterologous DNA in the genome.

In the first of several studies using single-molecule methods to investigate the RecA-dependent homology search process, Forget & Kowalczykowski (139) used single-molecule imaging and DNA micromanipulation to demonstrate that the 3D conformation of dsDNA in the vicinity of the filament is an important component of this kinetic search process (**Figure 6*a*,*b***; **Supplemental Videos 9 and 10**). When dsDNA was held in an extended conformation in an optical trap or surface-tethering experiment, pairing between preformed RecA nucleoprotein filaments and the homologous dsDNA was too rare to observe; however, when the dsDNA conformation was allowed to relax into a 3D random coil, pairing was efficient (**Figure 6*b***). Importantly, it was shown that when the end-to-end distance of the dsDNA was changed in a controlled manner by manipulating DNA dumbbells with an optical trap, the pairing efficiency monotonically increased as the dsDNA became more collapsed (**Figure 6*c***). The simplest interpretation of this observation is that to find homologous sequences efficiently, the RecA filament must make many simultaneous contacts with the dsDNA target via a process called intersegmental contact sampling, which is a form of molecular parallel processing (139). In other words, the homology

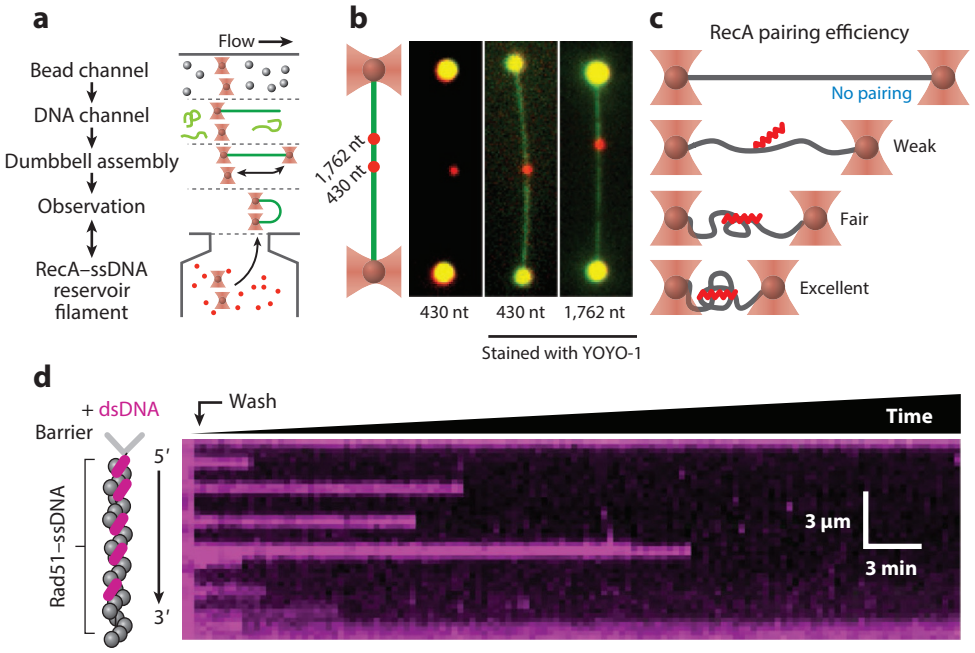

Figure 6

Homology search and recognition by RecA and Rad51. (*a*) Schematic of the experimental system used by Forget & Kowalczykowski (139) to manipulate single molecules of DNA to interrogate RecA-mediated homology search and pairing. (*b*) Two optical traps were used to manipulate the ends of a double-stranded DNA (dsDNA) molecule as it was incubated in a flow-free reservoir containing preassembled RecA–single-stranded DNA (ssDNA) filaments. After incubation, molecules were moved to an observation channel and imaged before and after staining with YOYO-1 and extending DNA-dumbbell. The length of the RecA–ssDNA nucleoprotein filament was varied: Pairings with 430 nucleotides (nt) and 1,762 nt homologous sequences are shown (139). (*c*) The frequency of stable pairing events increased monotonically as the end-to-end distance was reduced, leading the authors to propose a model of intersegmental contact sampling, in which a single filament engages with multiple sites and engages in a parallel-processing search strategy. (*d*) (*left*) Schematic used to measure recognition of homologous dsDNA by Rad51–ssDNA filaments, and a kymograph depicting several dsDNA molecules (*magenta*) bound to a Rad51–ssDNA filament (not visible) for the duration indicated (146). Panels *a* and *b* adapted from Reference 139 with permission from Nature Publishing Group. Panel *d* adapted from Reference 146 with permission from Elsevier.

search conducted by the RecA-ssDNA filament is not limited to a single target sequence per contact because it forms a filament on ssDNA, generated during DNA resection, that can be thousands of nucleotides in length. Therefore, the nucleoprotein filament comprises hundreds of independent searching segments tiled into a contiguous binding surface.

A classic theoretical analysis by Berg et al. (140) suggested that the optimal search process is driven by a combination of 3D collisions and 1D sliding. To determine whether RecA also employed 1D sliding to find its homologous site, single-molecule FRET was used to probe the dynamic fluctuations of RecA nucleoprotein filaments on short, oligonucleotide-length filaments and dsDNA targets (141, 142). Indeed, rapid fluctuations consistent with the sliding of the filament along the dsDNA were observed, with each filament sampling 60–300 bp per sliding event (142).

Thus, the RecA filament employs the same physical and statistical search strategy used by lac repressor: It uses both 1D and 3D diffusion to find homologous sequences. The major difference, however, is that the weighting of the preferred search mechanisms is inverted: Sequence-specific binding proteins primarily use local sliding to accelerate target searching, whereas the RecA filaments use massively parallel, intersegmental 3D sampling.

Recognition of Homologous DNA Occurs Through Microhomology Sampling, Excluding Heterologous DNA to Reduce Complexity

Despite these observations, the specific manner by which homologous DNA is recognized and heterologous DNA sequences are rejected by RecA and Rad51 remained qualitative. However, both modeling and recent single-molecule measurements have provided elegant and satisfying conclusions to this longstanding problem (143–145). In brief, homology is tested in successive groups of either two or three sets of nucleotide triplets held in the filament. A match of eight contiguous base pairs is sufficient to energetically define an initial homologous match, and it does so in a manner that is rapid and that kinetically discards any mismatched nascent sequences. This was demonstrated in a set of elegant experiments using a TIRF-based approach, in which Rad51-coated ssDNA was tethered between nanofabricated barriers and short, fluorescently labeled ds-DNA oligonucleotides were incubated with the filaments. The lifetimes of dsDNA molecules transiently paired with Rad51-ssDNA filaments were measured while the extent of heterology was varied (**Figure *6d***) (146). The oligonucleotides were designed to be largely nonhomologous, with only short tracts of microhomology. By measuring the position and lifetime of each molecule bound to the Rad51 filament, the authors determined that eight nucleotides of microhomology function as the fundamental unit of homology recognition, in remarkable agreement with the modeling (145). Notably, the pairing of the ninth nucleotide demarks the transition from search to pairing and strand exchange, and all subsequent contributions to free energy coincided with 3 nt increments, corresponding to the nucleotide triplets held within the filament (145, 146). Collectively, these experiments (139, 145, 146) demonstrate that RecA and Rad51 homology search uses both a reduction in complexity through microhomology sampling to kinetically and energetically discriminate against heterologous sequences and a reduction in dimensionality through intersegmental contact sampling.

Watching the Search Process in Living Cells

In bacterial cells, DNA is condensed and confined in a small volume through supercoiling. Imaging of RecA filaments in living *E. coli* cells demonstrates that the filaments span the entire length of a single bacteria cell and are capable of spanning both mother and daughter cells (147). Interestingly, many filaments appear to aggregate into bundles, although the precise nature of this bundling is poorly understood. Amazingly, using time-lapse super-resolution imaging, Lesterlin et al. (147) could watch the ends of filaments protruding from these bundles moving in real-time, thus monitoring RecA filament assembly, the time required for the homology search, the dwell time after an initial pairing event, and, finally, the time to filament disassembly. Filament assembly and disassembly were relatively fast, each occurring within about 15 minutes; however, the homology search and dwell time after pairing were each observed to take approximately 50 minutes. Interestingly, the RecA filaments appear to explore only a limited volume of the cell and are excluded from the bulk of the nucleoid (147). What this means, and how RecA overcomes this restriction, remain open and interesting questions.

THE END: MECHANICS OF HOLLIDAY JUNCTION MIGRATION, DISSOLUTION, AND RESOLUTION

In *E. coli*, branch migration and Holliday junction resolution are both catalyzed by a single, heterotrimeric machine, RuvABC. A tetramer of RuvA binds to a four-way HJ, recruiting the assembly of two hexamers of the translocase RuvB on two of the four arms. The two RuvB hexamers face each other across the junction, forming a novel dual pump that simultaneously reels in two arms of the junction as the other two arms are extruded (148). Single-molecule measurements of RuvAB translocation, made using magnetic tweezers, demonstrated that branch migration is processive, moving at a rate of approximately 50 bp/s (149). The RuvAB complex functions with RuvC, which is the prototypic endonuclease that recognizes and cleaves an HJ across the junction to produce both crossover and noncrossover products (15). Unfortunately, a detailed description of eukaryotic resolution and dissolution is beyond the scope of this review, and the study of these remarkably complex processes has not yet progressed to single-molecule analyses; however, we direct the interested reader to several excellent biochemical reviews on the subject (see 6, 15).

CONCLUSIONS AND FUTURE PERSPECTIVES

It is without doubt or controversy that we have learned much about the mechanism of DNA recombination during the last half century and, yet, so much remains to be learned. In this section, we restrict our comments to biochemical and biophysical questions. Starting at the beginning, much remains to be learned about the initiation of DNA recombination, especially in eukaryotes. The mechanism of initiation mediated by the RecQ helicase family of proteins remains largely unexplored and how the functions of these enzymes are controlled by macromolecular assembly remains a mystery. The associated nucleases involved are even more poorly understood. Are these helicases or nucleases "smart" enough to know when DNA resection has revealed DNA sequence homology (i.e., is there molecular feedback from the DNA pairing process that regulates the extent of resection), or is the process completely stochastic? Is RecBCD the only enzyme (or enzyme family member) to directly load its cognate DNA-pairing protein, RecA, onto ssDNA and thereby directly couple initiation with DNA pairing, or are the reported interactions of the eukaryotic resection helicases with RAD51 the tip of the proverbial interaction-and-loading iceberg, revealing that the actions of these enzymes are also coordinated with RAD51 loading (150)? And why are there so many RecQ helicases (151)?

Although the biochemical properties of RAD51 are similar to RecA (152), critical differences are worth noting. First, nucleotide exchange during the hydrolysis cycle appears to be much slower in RAD51, permitting the accumulation of adenosine diphosphate (ADP) and shifting the protein to its low-affinity state (153, 154). This raises the question of whether there are ADP exchange factors that function analogously to GDP exchange factors for G proteins. In fact, this may be a function of a subset of the RAD51 paralogs (155). Second, the net bias of Rad51 filament assembly is opposite to that of RecA, preferentially assembling in the $3' \rightarrow 5'$ direction (156). Whether this is the normal assembly bias of this protein or whether it is altered by proteins that interact with RAD51 to regulate the directionality of growth is also unknown. In this context, the role of the mediators remains obscure: Which aspect of filament dynamics is actually being regulated? Will the canonical ideas of filament assembly/disassembly that were developed from bacterial studies be extended to eukaryotes, or will new paradigms for regulations be discovered? We are willing to bet that new paradigms will be needed to understand the complexities demanded by more complex organisms. And why are there so many RAD51 paralogs (17)?

Of particular interest are how RAD51 searches for homology in the context of chromatin and how the physical organization (e.g., topologically associated domains) of the genome influences search and recombination bias. RAD51 has a higher affinity for dsDNA than RecA, possibly owing to the fact that in vivo Rad51 must search for homology on chromatin and thus requires a higher affinity in its secondary binding site to overcome competition with nucleosomes (156). Whether this causes Rad51 to become stuck more often at quasi-homologous sites due to the possibility of longer-lived mispaired intermediate complexes is also not known. And how are repair outcomes influenced by different chromatin states? To what extent do histone chaperones and chromatin-remodeling enzymes affect this process? How does chromatid cohesion impose sister recombination bias, and is this bias merely a consequence of physical proximity, or are other biochemical mechanisms at play? How does chromatin-associated RNA (e.g., R-loops or noncoding RNA) affect recombination? And why are there so many chromatin-remodeling complexes involved in recombination (157)? And although barely discussed, the resolution/dissolution decision is both mechanistically interesting and biologically important. The Holliday junction is a unique biological structure, and how it is migrated remains a bit of a mystery (6). How movement of the junction is coordinated with decantenation remains even more mysterious, especially for those who are topologically challenged. And why are there so many Holliday junction resolution nucleases (15)?

We suspect that a combination of biochemical reconstitution studies, genetic interrogation, single-molecule biophysical visualization, systems biology, and intracellular super-resolution imaging will make these questions seem trivial in the next decade.

DISCLOSURE STATEMENT

The authors are not aware of any affiliations, memberships, funding, or financial holdings that might be perceived as affecting the objectivity of this review.

ACKNOWLEDGMENTS

The research in S.C.K.'s laboratory was supported by grants from the US National Institutes of Health (GM41347, GM62653, GM64745, and CA154920) and from the US Department of Defense, Congressionally Directed Medical Research Programs' Breast Cancer Research Program (W81XWH-13-1-0322). When at UC Davis, J.C.B. was supported by National Institutes of Health Training Grant T32 GM007377. We are grateful to Dr. Wolf-Dietrich Heyer and the members of the S.C.K. laboratory for their reading of a draft of this manuscript.

LITERATURE CITED

1. Ciccia A, Elledge SJ. 2010. The DNA damage response: making it safe to play with knives. *Mol. Cell* 40:179–204
2. Drake JW, Charlesworth B, Charlesworth D, Crow JF. 1998. Rates of spontaneous mutation. *Genetics* 148:1667–86
3. Hoeijmakers JH. 2009. DNA damage, aging, and cancer. *N. Engl. J. Med.* 361:1475–85
4. Sanz MM, German J. 1993. In *GeneReviews*, ed. RA Pagon, MP Adam, HH Ardinger, SE Wallace, A Amemiya, et al. Seattle (WA)
5. Kottemann MC, Smogorzewska A. 2013. Fanconi anaemia and the repair of Watson and Crick DNA crosslinks. *Nature* 493:356–63
6. Bizard AH, Hickson ID. 2014. The dissolution of double Holliday junctions. *Cold Spring Harb. Perspect. Biol.* 6:a016477

7. Kogoma T. 1997. Stable DNA replication: interplay between DNA replication, homologous recombination, and transcription. *Microbiol. Mol. Biol. Rev.* 61:212–38
8. Kowalczykowski SC. 2000. Initiation of genetic recombination and recombination-dependent replication. *Trends Biochem. Sci.* 25:156–65
9. Kuzminov A. 1996. *Recombinational Repair of DNA Damage*. Austin, TX: RG Landes
10. Cox MM, Goodman MF, Kreuzer KN, Sherratt DJ, Sandler SJ, Marians KJ. 2000. The importance of repairing stalled replication forks. *Nature* 404:37–41
11. Vilenchik MM, Knudson AG. 2003. Endogenous DNA double-strand breaks: production, fidelity of repair, and induction of cancer. *PNAS* 100:12871–76
12. Bzymek M, Thayer NH, Oh SD, Kleckner N, Hunter N. 2010. Double Holliday junctions are intermediates of DNA break repair. *Nature* 464:937–41
13. Wolff S. 1977. Sister chromatid exchange. *Annu. Rev. Genet.* 11:183–201
14. Chaganti RS, Schonberg S, German J. 1974. A manyfold increase in sister chromatid exchanges in Bloom's syndrome lymphocytes. *PNAS* 71:4508–12
15. Wyatt HD, West SC. 2014. Holliday junction resolvases. *Cold Spring Harb. Perspect. Biol.* 6:a023192
16. Clark AJ, Margulies AD. 1965. Isolation and characterization of recombination-deficient mutants of *Escherichia coli* K12. *PNAS* 53:451–59
17. Kowalczykowski SC. 2015. An overview of the molecular mechanisms of recombinational DNA repair. *Cold Spring Harb Perspect. Biol.* 7:a016410
18. Heyer WD. 2015. Regulation of recombination and genomic maintenance. *Cold Spring Harb. Perspect. Biol.* 7:a016501
19. Amitani I, Liu B, Dombrowski CC, Baskin RJ, Kowalczykowski SC. 2010. Watching individual proteins acting on single molecules of DNA. *Methods Enzymol.* 472:261–91
20. Forget AL, Dombrowski CC, Amitani I, Kowalczykowski SC. 2013. Exploring protein–DNA interactions in 3D using in situ construction, manipulation and visualization of individual DNA dumbbells with optical traps, microfluidics and fluorescence microscopy. *Nat. Protoc.* 8:525–38
21. Bustamante C, Bryant Z, Smith SB. 2003. Ten years of tension: single-molecule DNA mechanics. *Nature* 421:423–27
22. Ha T, Kozlov AG, Lohman TM. 2012. Single-molecule views of protein movement on single-stranded DNA. *Annu. Rev. Biophys.* 41:295–319
23. van Oijen AM, Loparo JJ. 2010. Single-molecule studies of the replisome. *Annu. Rev. Biophys.* 39:429–48
24. Bustamante C, Cheng W, Mejia YX. 2011. Revisiting the central dogma one molecule at a time. *Cell* 144:480–97
25. Duzdevich D, Redding S, Greene EC. 2014. DNA dynamics and single-molecule biology. *Chem. Rev.* 114:3072–86
26. Perkins TT, Quake SR, Smith DE, Chu S. 1994. Relaxation of a single DNA molecule observed by optical microscopy. *Science* 264:822–26
27. Brewer LR, Bianco PR. 2008. Laminar flow cells for single-molecule studies of DNA–protein interactions. *Nat. Methods* 5:517–25
28. Bianco PR, Brewer LR, Corzett M, Balhorn R, Yeh Y, et al. 2001. Processive translocation and DNA unwinding by individual RecBCD enzyme molecules. *Nature* 409:374–78
29. Galletto R, Amitani I, Baskin RJ, Kowalczykowski SC. 2006. Direct observation of individual RecA filaments assembling on single DNA molecules. *Nature* 443:875–78
30. Liu B, Baskin RJ, Kowalczykowski SC. 2013. DNA unwinding heterogeneity by RecBCD results from static molecules able to equilibrate. *Nature* 500:482–85
31. Fordyce PM, Valentine MT, Block SM. 2008. Advances in surface-based assays for single molecules. In *Single-Molecule Techniques: A Laboratory Manual*, ed. P Selvin, T Ha, 20:431–460. Cold Spring Harbor, NY: Cold Spring Harb. Lab.
32. Ha T, Enderle T, Ogletree DF, Chemla DS, Selvin PR, Weiss S. 1996. Probing the interaction between two single molecules: fluorescence resonance energy transfer between a single donor and a single acceptor. *PNAS* 93:6264–68
33. Joo C, Balci H, Ishitsuka Y, Buranachai C, Ha T. 2008. Advances in single-molecule fluorescence methods for molecular biology. *Annu. Rev. Biochem.* 77:51–76

34. Léger JF, Romano G, Sarkar A, Robert J, Bourdieu L, et al. 1999. Structural transitions of a twisted and stretched DNA molecule. *Phys. Rev. Lett.* 83:1066–69
35. Neuman KC, Block SM. 2004. Optical trapping. *Rev. Sci. Instrum.* 75:2787–809
36. Zhou R, Kozlov AG, Roy R, Zhang J, Korolev S, et al. 2011. SSB functions as a sliding platform that migrates on DNA via reptation. *Cell* 146:222–32
37. Bryant Z, Oberstrass FC, Basu A. 2012. Recent developments in single-molecule DNA mechanics. *Curr. Opin. Struct. Biol.* 22:304–12
38. Dillingham MS, Kowalczykowski SC. 2008. RecBCD enzyme and the repair of double-stranded DNA breaks. *Microbiol. Mol. Biol. Rev.* 72:642–71
39. Singleton MR, Dillingham MS, Gaudier M, Kowalczykowski SC, Wigley DB. 2004. Crystal structure of RecBCD enzyme reveals a machine for processing DNA breaks. *Nature* 432:187–93
40. Dillingham MS, Spies M, Kowalczykowski SC. 2003. RecBCD enzyme is a bipolar DNA helicase. *Nature* 423:893–97
41. Taylor AF, Smith GR. 2003. RecBCD enzyme is a DNA helicase with fast and slow motors of opposite polarity. *Nature* 423:889–93
42. Smith GR, Kunes SM, Schultz DW, Taylor A, Triman KL. 1981. Structure of chi hotspots of generalized recombination. *Cell* 24:429–36
43. Arnold DA, Handa N, Kobayashi I, Kowalczykowski SC. 2000. A novel, 11 nucleotide variant of χ, χ*: one of a class of sequences defining the *Escherichia coli* recombination hotspot χ. *J. Mol. Biol.* 300:469–79
44. Handa N, Yang L, Dillingham MS, Kobayashi I, Wigley DB, Kowalczykowski SC. 2012. Molecular determinants responsible for recognition of the single-stranded DNA regulatory sequence, χ, by RecBCD enzyme. *PNAS* 109:8901–6
45. Yang L, Handa N, Liu B, Dillingham MS, Wigley DB, Kowalczykowski SC. 2012. Alteration of χ recognition by RecBCD reveals a regulated molecular latch and suggests a channel-bypass mechanism for biological control. *PNAS* 109:8907–12
46. Stahl FW. 2005. Chi: A little sequence controls a big enzyme. *Genetics* 170:487–93
47. Spies M, Bianco PR, Dillingham MS, Handa N, Baskin RJ, Kowalczykowski SC. 2003. A molecular throttle: The recombination hotspot χ controls DNA translocation by the RecBCD helicase. *Cell* 114:647–54
48. Dixon DA, Kowalczykowski SC. 1991. Homologous pairing in vitro stimulated by the recombination hotspot, Chi. *Cell* 66:361–71
49. Dixon DA, Kowalczykowski SC. 1993. The recombination hotspot χ is a regulatory sequence that acts by attenuating the nuclease activity of the *E. coli* RecBCD enzyme. *Cell* 73:87–96
50. Dillingham MS, Webb MR, Kowalczykowski SC. 2005. Bipolar DNA translocation contributes to highly processive DNA unwinding by RecBCD enzyme. *J. Biol. Chem.* 280:37069–77
51. Spies M, Dillingham MS, Kowalczykowski SC. 2005. Translocation by the RecB motor is an absolute requirement for χ–recognition and RecA protein loading by RecBCD enzyme. *J. Biol. Chem.* 280:37078–87
52. Handa N, Bianco PR, Baskin RJ, Kowalczykowski SC. 2005. Direct visualization of RecBCD movement reveals cotranslocation of the RecD motor after χ recognition. *Mol. Cell* 17:745–50
53. Spies M, Amitani I, Baskin RJ, Kowalczykowski SC. 2007. RecBCD enzyme switches lead motor subunits in response to χ recognition. *Cell* 131:694–705
54. Wang J, Chen R, Julin DA. 2000. A single nuclease active site of the *Escherichia coli* RecBCD enzyme catalyzes single-stranded DNA degradation in both directions. *J. Biol. Chem.* 275:507–13
55. Anderson DG, Kowalczykowski SC. 1997. The translocating RecBCD enzyme stimulates recombination by directing RecA protein onto ssDNA in a χ-regulated manner. *Cell* 90:77–86
56. Arnold DA, Kowalczykowski SC. 2000. Facilitated loading of RecA protein is essential to recombination by RecBCD enzyme. *J. Biol. Chem.* 275:12261–65
57. Spies M, Kowalczykowski SC. 2006. The RecA binding locus of RecBCD is a general domain for recruitment of DNA strand exchange proteins. *Mol. Cell* 21:573–80
58. Levy A, Goren MG, Yosef I, Auster O, Manor M, et al. 2015. CRISPR adaptation biases explain preference for acquisition of foreign DNA. *Nature* 520:505–10

59. Finkelstein IJ, Visnapuu ML, Greene EC. 2010. Single-molecule imaging reveals mechanisms of protein disruption by a DNA translocase. *Nature* 468:983–87
60. Eggleston AK, O'Neill TE, Bradbury EM, Kowalczykowski SC. 1995. Unwinding of nucleosomal DNA by a DNA helicase. *J. Biol. Chem.* 270:2024–31
61. Chow KH, Courcelle J. 2007. RecBCD and RecJ/RecQ initiate DNA degradation on distinct substrates in UV-irradiated *Escherichia coli*. *Radiat. Res.* 168:499–506
62. Pennington JM, Rosenberg SM. 2007. Spontaneous DNA breakage in single living *Escherichia coli* cells. *Nat. Genet.* 39:797–802
63. Morimatsu K, Kowalczykowski SC. 2014. RecQ helicase and RecJ nuclease provide complementary functions to resect DNA for homologous recombination. *PNAS* 111:E5133–42
64. Harmon FG, Kowalczykowski SC. 2001. Biochemical characterization of the DNA helicase activity of the *Escherichia coli* RecQ helicase. *J. Biol. Chem.* 276:232–43
65. Shereda RD, Reiter NJ, Butcher SE, Keck JL. 2009. Identification of the SSB binding site on *E. coli* RecQ reveals a conserved surface for binding SSB's C terminus. *J. Mol. Biol.* 386:612–25
66. Rad B, Kowalczykowski SC. 2012. Translocation of *E. coli* RecQ helicase on single-stranded DNA. *Biochemistry* 51:2921–29
67. Rad B, Kowalczykowski SC. 2012. Efficient coupling of ATP hydrolysis to translocation by RecQ helicase. *PNAS* 109:1443–48
68. Rad B, Forget AL, Baskin RJ, Kowalczykowski SC. 2015. Single-molecule visualization of RecQ helicase reveals DNA melting, nucleation, and assembly are required for processive DNA unwinding. *PNAS* 112(50):E6851–61
69. Byrd AK, Raney KD. 2015. Fine tuning of a DNA fork by the RecQ helicase. *PNAS* 112:15263–64
70. Symington LS. 2014. End resection at double-strand breaks: mechanism and regulation. *Cold Spring Harb. Perspect. Biol.* 6:a016436
71. Cannavo E, Cejka P. 2014. Sae2 promotes dsDNA endonuclease activity within Mre11–Rad50–Xrs2 to resect DNA breaks. *Nature* 514:122–25
72. Cejka P, Kowalczykowski SC. 2010. The full-length *Saccharomyces cerevisiae* Sgs1 protein is a vigorous DNA helicase that preferentially unwinds Holliday junctions. *J. Biol. Chem.* 285:8290–301
73. Masuda-Sasa T, Imamura O, Campbell JL. 2006. Biochemical analysis of human Dna2. *Nucleic Acids Res.* 34:1865–75
74. Cejka P, Cannavo E, Polaczek P, Masuda-Sasa T, Pokharel S, et al. 2010. DNA end resection by Dna2–Sgs1–RPA and its stimulation by Top3–Rmi1 and Mre11–Rad50–Xrs2. *Nature* 467:112–16
75. Niu H, Chung WH, Zhu Z, Kwon Y, Zhao W, et al. 2010. Mechanism of the ATP-dependent DNA end-resection machinery from *Saccharomyces cerevisiae*. *Nature* 467:108–11
76. Levikova M, Klaue D, Seidel R, Cejka P. 2013. Nuclease activity of *Saccharomyces cerevisiae* Dna2 inhibits its potent DNA helicase activity. *PNAS* 110:E1992–2001
77. Cannavo E, Cejka P, Kowalczykowski SC. 2013. Relationship of DNA degradation by *Saccharomyces cerevisiae* exonuclease 1 and its stimulation by RPA and Mre11–Rad50–Xrs2 to DNA end resection. *PNAS* 110:E1661–68
78. Nimonkar AV, Genschel J, Kinoshita E, Polaczek P, Campbell JL, et al. 2011. BLM–DNA2–RPA–MRN and EXO1–BLM–RPA–MRN constitute two DNA end resection machineries for human DNA break repair. *Genes Dev.* 25:350–62
79. Nimonkar AV, Ozsoy AZ, Genschel J, Modrich P, Kowalczykowski SC. 2008. Human exonuclease 1 and BLM helicase interact to resect DNA and initiate DNA repair. *PNAS* 105:16906–11
80. Shim EY, Chung WH, Nicolette ML, Zhang Y, Davis M, et al. 2010. *Saccharomyces cerevisiae* Mre11/Rad50/Xrs2 and Ku proteins regulate association of Exo1 and Dna2 with DNA breaks. *EMBO J.* 29:3370–80
81. Shereda RD, Kozlov AG, Lohman TM, Cox MM, Keck JL. 2008. SSB as an organizer/mobilizer of genome maintenance complexes. *Crit. Rev. Biochem. Mol. Biol.* 43:289–318
82. Raghunathan S, Kozlov AG, Lohman TM, Waksman G. 2000. Structure of the DNA binding domain of *E. coli* SSB bound to ssDNA. *Nat. Struct. Biol.* 7:648–52

83. Kowalczykowski SC, Krupp RA. 1987. Effects of *Escherichia coli* SSB protein on the single-stranded DNA-dependent ATPase activity of *Escherichia coli* RecA protein: evidence that SSB protein facilitates the binding of RecA protein to regions of secondary structure within single-stranded DNA. *J. Mol. Biol.* 193:97–113
84. Roy R, Kozlov AG, Lohman TM, Ha T. 2009. SSB protein diffusion on single-stranded DNA stimulates RecA filament formation. *Nature* 461:1092–97
85. Roy R, Kozlov AG, Lohman TM, Ha T. 2007. Dynamic structural rearrangements between DNA binding modes of *E. coli* SSB protein. *J. Mol. Biol.* 369:1244–57
86. Lee KS, Marciel AB, Kozlov AG, Schroeder CM, Lohman TM, Ha T. 2014. Ultrafast redistribution of *E. coli* SSB along long single-stranded DNA via intersegment transfer. *J. Mol. Biol.* 426:2413–21
87. Kozlov AG, Lohman TM. 2002. Kinetic mechanism of direct transfer of *Escherichia coli* SSB tetramers between single-stranded DNA molecules. *Biochemistry* 41:11611–27
88. Bell JC, Liu B, Kowalczykowski SC. 2015. Imaging and energetics of single SSB-ssDNA molecules reveal intramolecular condensation and insight into RecOR function. *eLife* 4:e08646
89. Chen R, Wold MS. 2014. Replication protein A: single-stranded DNA's first responder: Dynamic DNA-interactions allow replication protein A to direct single-strand DNA intermediates into different pathways for synthesis or repair. *BioEssays* 36:1156–61
90. Wold MS. 1997. Replication protein A: a heterotrimeric, single-stranded DNA-binding protein required for eukaryotic DNA metabolism. *Annu. Rev. Biochem.* 66:61–92
91. Bochkarev A, Bochkareva E, Frappier L, Edwards AM. 1999. The crystal structure of the complex of replication protein A subunits RPA32 and RPA14 reveals a mechanism for single-stranded DNA binding. *EMBO J.* 18:4498–504
92. Bochkarev A, Pfuetzner RA, Edwards AM, Frappier L. 1997. Structure of the single-stranded-DNA-binding domain of replication protein A bound to DNA. *Nature* 385:176–81
93. Nguyen B, Sokoloski J, Galletto R, Elson EL, Wold MS, Lohman TM. 2014. Diffusion of human replication protein A along single-stranded DNA. *J. Mol. Biol.* 426:3246–61
94. Gibb B, Ye LF, Gergoudis SC, Kwon Y, Niu H, et al. 2014. Concentration-dependent exchange of replication protein A on single-stranded DNA revealed by single-molecule imaging. *PLOS ONE* 9:e87922
95. Kunzelmann S, Morris C, Chavda AP, Eccleston JF, Webb MR. 2010. Mechanism of interaction between single-stranded DNA binding protein and DNA. *Biochemistry* 49:843–52
96. Bell JC, Plank JL, Dombrowski CC, Kowalczykowski SC. 2012. Direct imaging of RecA nucleation and growth on single molecules of SSB-coated ssDNA. *Nature* 491:274–78
97. Sing CE, Olvera de la Cruz M, Marko JF. 2014. Multiple-binding-site mechanism explains concentration-dependent unbinding rates of DNA-binding proteins. *Nucleic Acids Res.* 42:3783–91
98. Bell JC, Kowalczykowski SC. 2015. RecA: regulation and mechanism of a molecular search engine. *Trends Biochem. Sci.* In press
99. Umezu K, Chi NW, Kolodner RD. 1993. Biochemical interaction of the *Escherichia coli* RecF, RecO, and RecR proteins with RecA protein and single-stranded DNA binding protein. *PNAS* 90:3875–79
100. Kowalczykowski SC, Clow J, Somani R, Varghese A. 1987. Effects of the *Escherichia coli* SSB protein on the binding of *Escherichia coli* RecA protein to single-stranded DNA: demonstration of competitive binding and the lack of a specific protein–protein interaction. *J. Mol. Biol.* 193:81–95
101. Wegner A, Engel J. 1975. Kinetics of the cooperative association of actin to actin filaments. *Biophys. Chem.* 3:215–25
102. Bryan J. 1976. A quantitative analysis of microtubule elongation. *J. Cell Biol.* 71:749–67
103. Joo C, McKinney SA, Nakamura M, Rasnik I, Myong S, Ha T. 2006. Real-time observation of RecA filament dynamics with single monomer resolution. *Cell* 126:515–27
104. Morimatsu K, Kowalczykowski SC. 2003. RecFOR proteins load RecA protein onto gapped DNA to accelerate DNA strand exchange: a universal step of recombinational repair. *Mol. Cell* 11:1337–47
105. Blanar MA, Sandler SJ, Armengod ME, Ream LW, Clark AJ. 1984. Molecular analysis of the recF gene of *Escherichia coli*. *PNAS* 81:4622–26
106. Morimatsu K, Wu Y, Kowalczykowski SC. 2012. RecFOR proteins target RecA protein to a DNA gap with either DNA or RNA at the 5′ terminus: implication for repair of stalled replication forks. *J. Biol. Chem.* 287:35621–30

107. Sung P. 1997. Function of yeast Rad52 protein as a mediator between replication protein A and the Rad51 recombinase. *J. Biol. Chem.* 272:28194–97
108. Shinohara A, Ogawa T. 1998. Stimulation by Rad52 of yeast Rad51-mediated recombination. *Nature* 391:404–7
109. New JH, Sugiyama T, Zaitseva E, Kowalczykowski SC. 1998. Rad52 protein stimulates DNA strand exchange by Rad51 and replication protein A. *Nature* 391:407–10
110. Sugiyama T, New JH, Kowalczykowski SC. 1998. DNA annealing by RAD52 protein is stimulated by specific interaction with the complex of replication protein A and single-stranded DNA. *PNAS* 95:6049–54
111. Gibb B, Ye LF, Kwon Y, Niu H, Sung P, Greene EC. 2014. Protein dynamics during presynaptic-complex assembly on individual single-stranded DNA molecules. *Nat. Struct. Mol. Biol.* 21:893–900
112. Sasanuma H, Tawaramoto MS, Lao JP, Hosaka H, Sanda E, et al. 2013. A new protein complex promoting the assembly of Rad51 filaments. *Nat. Commun.* 4:1676
113. Fortin GS, Symington LS. 2002. Mutations in yeast Rad51 that partially bypass the requirement for Rad55 and Rad57 in DNA repair by increasing the stability of Rad51–DNA complexes. *EMBO J.* 21:3160–70
114. Fung CW, Mozlin AM, Symington LS. 2009. Suppression of the double-strand-break-repair defect of the *Saccharomyces cerevisiae rad57* mutant. *Genetics* 181:1195–206
115. Liu J, Renault L, Veaute X, Fabre F, Stahlberg H, Heyer WD. 2011. Rad51 paralogues Rad55-Rad57 balance the antirecombinase Srs2 in Rad51 filament formation. *Nature* 479:245–48
116. Bernstein KA, Reid RJ, Sunjevaric I, Demuth K, Burgess RC, Rothstein R. 2011. The Shu complex, which contains Rad51 paralogues, promotes DNA repair through inhibition of the Srs2 anti-recombinase. *Mol. Biol. Cell* 22:1599–607
117. Shor E, Weinstein J, Rothstein R. 2005. A genetic screen for top3 suppressors in *Saccharomyces cerevisiae* identifies SHU_1, SHU_2, PSY_3 and CSM_2: four genes involved in error-free DNA repair. *Genetics* 169:1275–89
118. Gaines WA, Godin SK, Kabbinavar FF, Rao T, VanDemark AP, et al. 2015. Promotion of presynaptic filament assembly by the ensemble of *S. cerevisiae* Rad51 paralogues with Rad52. *Nat. Commun.* 6:7834
119. Jensen RB, Carreira A, Kowalczykowski SC. 2010. Purified human BRCA2 stimulates RAD51-mediated recombination. *Nature* 467:678–83
120. Liu J, Doty T, Gibson B, Heyer WD. 2010. Human BRCA2 protein promotes RAD51 filament formation on RPA-covered single-stranded DNA. *Nat. Struct. Mol. Biol.* 17:1260–62
121. Wong AK, Pero R, Ormonde PA, Tavtigian SV, Bartel PL. 1997. RAD51 interacts with the evolutionarily conserved BRC motifs in the human breast cancer susceptibility gene *brca2*. *J. Biol. Chem.* 272:31941–44
122. Bignell G, Micklem G, Stratton MR, Ashworth A, Wooster R. 1997. The BRC repeats are conserved in mammalian BRCA2 proteins. *Hum. Mol. Genet.* 6:53–58
123. Hilario J, Amitani I, Baskin RJ, Kowalczykowski SC. 2009. Direct imaging of human Rad51 nucleoprotein dynamics on individual DNA molecules. *PNAS* 106:361–68
124. Rajendra E, Venkitaraman AR. 2010. Two modules in the BRC repeats of BRCA2 mediate structural and functional interactions with the RAD51 recombinase. *Nucleic Acids Res.* 38:82–96
125. Carreira A, Hilario J, Amitani I, Baskin RJ, Shivji MK, et al. 2009. The BRC repeats of BRCA2 modulate the DNA-binding selectivity of RAD51. *Cell* 136:1032–43
126. Shivji MK, Mukund SR, Rajendra E, Chen S, Short JM, et al. 2009. The BRC repeats of human BRCA2 differentially regulate RAD51 binding on single- versus double-stranded DNA to stimulate strand exchange. *PNAS* 106:13254–59
127. Carreira A, Kowalczykowski SC. 2011. Two classes of BRC repeats in BRCA2 promote RAD51 nucleoprotein filament function by distinct mechanisms. *PNAS* 108:10448–53
128. Shahid T, Soroka J, Kong EH, Malivert L, McIlwraith MJ, et al. 2014. Structure and mechanism of action of the BRCA2 breast cancer tumor suppressor. *Nat. Struct. Mol. Biol.* 21:962–68
129. Reuter M, Zelensky A, Smal I, Meijering E, van Cappellen WA, et al. 2014. BRCA2 diffuses as oligomeric clusters with RAD51 and changes mobility after DNA damage in live cells. *J. Cell Biol.* 207:599–613

130. Zhao W, Vaithiyalingam S, San Filippo J, Maranon DG, Jimenez-Sainz J, et al. 2015. Promotion of BRCA2-dependent homologous recombination by DSS1 via RPA targeting and DNA mimicry. *Mol. Cell* 59:176–87
131. Prakash R, Zhang Y, Feng W, Jasin M. 2015. Homologous recombination and human health: the roles of BRCA1, BRCA2, and associated proteins. *Cold Spring Harb. Perspect. Biol.* 7:a016600
132. Martinez JS, von Nicolai C, Kim T, Ehlen A, Mazin AV, et al. 2016. BRCA2 regulates DMC1-mediated recombination through the BRC repeats. *PNAS.* In press. doi: 10.1073/pnas.1601691113
133. Haurwitz RE, Jinek M, Wiedenheft B, Zhou K, Doudna JA. 2010. Sequence- and structure-specific RNA processing by a CRISPR endonuclease. *Science* 329:1355–58
134. Kowalczykowski SC. 1991. Biochemistry of genetic recombination: energetics and mechanism of DNA strand exchange. *Annu. Rev. Biophys. Biophys. Chem.* 20:539–75
135. Kowalczykowski SC. 1991. Biochemical and biological function of *Escherichia coli* RecA protein: behavior of mutant RecA proteins. *Biochimie* 73:289–304
136. Chen Z, Yang H, Pavletich NP. 2008. Mechanism of homologous recombination from the RecA–ssDNA/dsDNA structures. *Nature* 453:489–94
137. Kowalczykowski SC. 2008. Structural biology: snapshots of DNA repair. *Nature* 453:463–66
138. Mazin AV, Kowalczykowski SC. 1996. The specificity of the secondary DNA binding site of RecA protein defines its role in DNA strand exchange. *PNAS* 93:10673–78
139. Forget AL, Kowalczykowski SC. 2012. Single-molecule imaging of DNA pairing by RecA reveals a three-dimensional homology search. *Nature* 482:423–27
140. Berg OG, Winter RB, von Hippel PH. 1981. Diffusion-driven mechanisms of protein translocation on nucleic acids. 1. Models and theory. *Biochemistry* 20:6929–48
141. Ragunathan K, Joo C, Ha T. 2011. Real-time observation of strand exchange reaction with high spatiotemporal resolution. *Structure* 19:1064–73
142. Ragunathan K, Liu C, Ha T. 2012. RecA filament sliding on DNA facilitates homology search. *eLife* 1:e00067
143. Saladin A, Amourda C, Poulain P, Ferey N, Baaden M, et al. 2010. Modeling the early stage of DNA sequence recognition within RecA nucleoprotein filaments. *Nucleic Acids Res.* 38:6313–23
144. Savir Y, Tlusty T. 2010. RecA-mediated homology search as a nearly optimal signal detection system. *Mol. Cell* 40:388–96
145. Danilowicz C, Yang D, Kelley C, Prevost C, Prentiss M. 2015. The poor homology stringency in the heteroduplex allows strand exchange to incorporate desirable mismatches without sacrificing recognition in vivo. *Nucleic Acids Res.* 43:6473–85
146. Qi Z, Redding S, Lee JY, Gibb B, Kwon Y, et al. 2015. DNA sequence alignment by microhomology sampling during homologous recombination. *Cell* 160:856–69
147. Lesterlin C, Ball G, Schermelleh L, Sherratt DJ. 2014. RecA bundles mediate homology pairing between distant sisters during DNA break repair. *Nature* 506:249–53
148. Yu X, West SC, Egelman EH. 1997. Structure and subunit composition of the RuvAB–Holliday junction complex. *J. Mol. Biol.* 266:217–22
149. Dawid A, Croquette V, Grigoriev M, Heslot F. 2004. Single-molecule study of RuvAB-mediated Holliday-junction migration. *PNAS* 101:11611–16
150. Wu L, Davies SL, Levitt NC, Hickson ID. 2001. Potential role for the BLM helicase in recombinational repair via a conserved interaction with RAD51. *J. Biol. Chem.* 276:19375–81
151. Hickson ID. 2003. RecQ helicases: caretakers of the genome. *Nat. Rev. Cancer* 3:169–78
152. Bianco PR, Tracy RB, Kowalczykowski SC. 1998. DNA strand exchange proteins: a biochemical and physical comparison. *Front. Biosci.* 3:D570–603
153. Bugreev DV, Mazin AV. 2004. Ca^{2+} activates human homologous recombination protein Rad51 by modulating its ATPase activity. *PNAS* 101:9988–93
154. Tombline G, Shim KS, Fishel R. 2002. Biochemical characterization of the human RAD51 protein. II. Adenosine nucleotide binding and competition. *J. Biol. Chem.* 277:14426–33
155. Shim KS, Schmutte C, Tombline G, Heinen CD, Fishel R. 2004. hXRCC2 enhances ADP/ATP processing and strand exchange by hRAD51. *J. Biol. Chem.* 279:30385–94

156. Sung P, Robberson DL. 1995. DNA strand exchange mediated by a RAD51–ssDNA nucleoprotein filament with polarity opposite to that of RecA. *Cell* 82:453–61
157. Szekvolgyi L, Ohta K, Nicolas A. 2015. Initiation of meiotic homologous recombination: flexibility, impact of histone modifications, and chromatin remodeling. *Cold Spring Harb. Perspect. Biol.* 7:a016527
158. Pagon RA, Adam MP, Ardinger HH, Wallace SE, Amemiya A, et al., eds. 1993–2015. *GeneReviews*. Seattle, WA: Univ. Wash. **http://www.ncbi.nlm.nih.gov/books/NBK1116/**
159. Wang AT, Kim T, Wagner JE, Conti BA, Lach FP, et al. 2015. A dominant mutation in human RAD51 reveals its function in DNA interstrand crosslink repair independent of homologous recombination. *Mol. Cell* 59:478–90
160. Alter BP, Kupfer G. Fanconi anemia. 2002. See Ref. 158, **http://www.ncbi.nlm.nih.gov/books/NBK1401/**, updated Feb. 7, 2013
161. Sanz MM, German J. Bloom's syndrome. 2006. See Ref. 158, **http://www.ncbi.nlm.nih.gov/books/NBK1398/**, updated Mar. 28, 2013
162. Varon R, Demuth I, Digweed M. Nijmegen breakage syndrome. 1999. See Ref. 158, **http://www.ncbi.nlm.nih.gov/books/NBK1176/**, updated May 8, 2014
163. Petrucelli N, Daly MB, Feldman GL. *BRCA1* and *BRCA2* hereditary breast and ovarian cancer. 1998. See Ref. 158, **http://www.ncbi.nlm.nih.gov/books/NBK1247/**, updated Sep. 26, 2013
164. Cybulski C, Carrot-Zhang J, Kluzniak W, Rivera B, Kashyap A, et al. 2015. Germline RECQL mutations are associated with breast cancer susceptibility. *Nat. Genet.* 47:643–46
165. Sun J, Wang Y, Xia Y, Xu Y, Ouyang T, et al. 2015. Mutations in RECQL gene are associated with predisposition to breast cancer. *PLOS Genet.* 11:e1005228
166. Oshima J, Martin GM, Hisama FM. Werner syndrome. 2002. See Ref. 158, **http://www.ncbi.nlm.nih.gov/books/NBK1514/**, updated Mar. 27, 2014
167. Croteau DL, Popuri V, Opresko PL, Bohr VA. 2014. Human RecQ helicases in DNA repair, recombination, and replication. *Annu. Rev. Biochem.* 83:519–52
168. Gatti R. Ataxia–telangiectasia. 1999. See Ref. 158, **http://www.ncbi.nlm.nih.gov/books/NBK26468/**, updated Mar. 11, 2010
169. Wang LL, Plon SE. Rothmund–Thomson syndrome. 1999. See Ref. 158, **http://www.ncbi.nlm.nih.gov/books/NBK1237/**, updated June 6, 2013
170. Harmon FG, Brockman JP, Kowalczykowski SC. 2003. RecQ helicase stimulates both DNA catenation and changes in DNA topology by topoisomerase II. *J. Biol. Chem.* 278:42668–78
171. Galletto RG, Kowalczykowski SC. 2007. RecA. *Curr. Biol.* 17:R395–97